Dosimetry of ^{125}I and ^{103}Pd COMS eye plaques for intraocular tumors: Report of Task Group 129 by the AAPM and ABS

Sou-Tung Chiu-Tsao[a)]
Quality MediPhys LLC, Denville, New Jersey 07834

Melvin A. Astrahan
Department of Radiation Oncology, University of Southern California, Los Angeles, California 90033

Paul T. Finger
The New York Eye Cancer Center, New York, New York 10065

David S. Followill
Radiological Physics Center, University of Texas M.D. Anderson Cancer Center, Houston, Texas 77030

Ali S. Meigooni
Department of Radiation Oncology, Comprehensive Cancer Center of Nevada, Las Vegas, Nevada 89169

Christopher S. Melhus
Department of Radiation Oncology, Tufts University School of Medicine, Boston, Massachusetts 02111

Firas Mourtada
Department of Radiation Oncology, Helen F. Graham Cancer Center, Christiana Health Care System, Newark, Delaware 19713

Mary E. Napolitano
Physics, Elekta Inc., Norcross, Georgia 30092

Ravinder Nath
Department of Therapeutic Radiology, Yale University School of Medicine, New Haven, Connecticut 06510

Mark J. Rivard
Department of Radiation Oncology, Tufts University School of Medicine, Boston, Massachusetts 02111

D. W. O. Rogers and Rowan M. Thomson
Department of Physics, Carleton University, Ottawa K1S 5B6 Canada

(Received 2 May 2012; revised 14 August 2012; accepted for publication 14 August 2012; published 24 September 2012)

Dosimetry of eye plaques for ocular tumors presents unique challenges in brachytherapy. The challenges in accurate dosimetry are in part related to the steep dose gradient in the tumor and critical structures that are within millimeters of radioactive sources. In most clinical applications, calculations of dose distributions around eye plaques assume a homogenous water medium and full scatter conditions. Recent Monte Carlo (MC)-based eye-plaque dosimetry simulations have demonstrated that the perturbation effects of heterogeneous materials in eye plaques, including the gold-alloy backing and Silastic insert, can be calculated with reasonable accuracy. Even additional levels of complexity introduced through the use of gold foil "seed-guides" and custom-designed plaques can be calculated accurately using modern MC techniques. Simulations accounting for the aforementioned complexities indicate dose discrepancies exceeding a factor of ten to selected critical structures compared to conventional dose calculations. Task Group 129 was formed to review the literature; re-examine the current dosimetry calculation formalism; and make recommendations for eye-plaque dosimetry, including evaluation of brachytherapy source dosimetry parameters and heterogeneity correction factors. A literature review identified modern assessments of dose calculations for Collaborative Ocular Melanoma Study (COMS) design plaques, including MC analyses and an intercomparison of treatment planning systems (TPS) detailing differences between homogeneous and heterogeneous plaque calculations using the American Association of Physicists in Medicine (AAPM) TG-43U1 brachytherapy dosimetry formalism and MC techniques. This review identified that a commonly used prescription dose of 85 Gy at 5 mm depth in homogeneous medium delivers about 75 Gy and 69 Gy at the same 5 mm depth for specific ^{125}I and ^{103}Pd sources, respectively, when accounting for COMS plaque heterogeneities. Thus, the adoption of heterogeneous dose calculation methods in clinical practice would result in dose differences $>10\%$ and warrant a careful evaluation of the corresponding changes in prescription doses. Doses to normal ocular structures vary with choice of radionuclide,

plaque location, and prescription depth, such that further dosimetric evaluations of the adoption of MC-based dosimetry methods are needed. The AAPM and American Brachytherapy Society (ABS) recommend that clinical medical physicists should make concurrent estimates of heterogeneity-corrected delivered dose using the information in this report's tables to prepare for brachytherapy TPS that can account for material heterogeneities and for a transition to heterogeneity-corrected prescriptive goals. It is recommended that brachytherapy TPS vendors include material heterogeneity corrections in their systems and take steps to integrate planned plaque localization and image guidance. In the interim, before the availability of commercial MC-based brachytherapy TPS, it is recommended that clinical medical physicists use the line-source approximation in homogeneous water medium and the 2D AAPM TG-43U1 dosimetry formalism and brachytherapy source dosimetry parameter datasets for treatment planning calculations. Furthermore, this report includes quality management program recommendations for eye-plaque brachytherapy. © *2012 American Association of Physicists in Medicine*. [http://dx.doi.org/10.1118/1.4749933]

Key words: brachytherapy, eye plaque, COMS, dosimetry, TG-43, Monte Carlo, heterogeneities

TABLE OF CONTENTS

I. INTRODUCTION

Melanoma is the most common primary intraocular cancer arising from the uveal layer, which includes the choroid, ciliary body, and iris. There are about 2500 annual cases of uveal melanoma and 350 cases of retinoblastoma in the United States and about double that including Europe, Russia, and Australia. Brachytherapy of choroidal melanoma using radon seeds was first reported in 1930.[1] Many different radionuclides, including ^{125}I, ^{103}Pd, ^{131}Cs, ^{192}Ir, ^{60}Co, ^{90}Sr, ^{198}Au, and ^{106}Ru/^{106}Rh, among others, and various designs of eye plaques have been used in the brachytherapy of choroidal melanoma.[2–4] External beam techniques such as proton,[5–9] helium-ion,[10] and Gamma Knife[11] have also been employed.[3] Choice of radiation modality and prescribed dose can influence local tumor control, resultant visual acuity, eye retention, and cosmetic results. Because the eye is a small structure (25 mm–30 mm in diameter), the ocular dose distribution can be highly sensitive to the intrinsic assumptions of the dose calculation method. Consequently, characterization of radiation interactions for eye plaque dosimetry is critical in determining location and incidence of side-effects.[12,13]

In addition to its use in treating ocular melanomas, plaque brachytherapy has been used for retinoblastoma, choroidal hemangioma, select choroidal metastases, and exudative macular degeneration.[3,14] In comparison to enucleation (removal of eye), plaque brachytherapy offers equivalent tumor control while allowing eye preservation and vision retention.[13] However, due to different techniques and sources used in various institutions, there was little consensus about the treatment approach for this disease before 1985. In 1985, the Collaborative Ocular Melanoma Study (COMS) was created as a multi-institutional cooperative clinical trial sponsored by the National Eye Institute of the National Institutes of Health (Bethesda, MD). The COMS group standardized methods of plaque brachytherapy for choroidal melanomas and conducted two prospective randomized clinical trials.[15]

One trial of the COMS compared 20 Gy (4 Gy × 5 daily fractions) of external-beam radiotherapy prior to enucleation to no irradiation prior to enucleation. Patients eligible for inclusion in this "large choroidal melanoma study" had tumors with an apical height >10 mm or a maximal tumor basal dimension >16 mm. The COMS found that 20 Gy of preoperative external-beam radiotherapy did not improve survival.[16] The second COMS trial compared enucleation against a minimum of 100 Gy of ^{125}I plaque radiation therapy for medium-sized choroidal melanomas.[17–19] Medium-sized melanomas were defined as having an apical height from 2.5 mm to 10 mm and a maximal tumor basal dimension of ≤16 mm.[15] Here, the COMS found no survival differences. Thus, brachytherapy with ^{125}I eye plaques was confirmed to be as effective as enucleation for medium-sized choroidal melanoma, with the added advantages of eye and vision preservation.[18,19] The most recent publications on trial outcomes are in COMS Report No. 24 (2004) and Report No. 28 (2006).[16,19] In the COMS trials, the original dose prescription of 100 Gy was based upon dosimetry formalism and data before the report of Task Group 43 (TG-43) of the AAPM and was revised in November 1996 to 85 Gy[20–22] to give the same effective dose when using the TG-43 dosimetry formalism and parameters.[23] The standard eye plaques of COMS design (COMS-plaques) were initially designed with diameters from 12 mm to 20 mm in 2-mm increments.[24,25] Currently available COMS-style plaques with diameters of 10 mm and 22 mm were not part of the COMS study.

In 1986, the COMS recognized the uncertainties in accurate determination of dose distributions around the eye plaques. COMS required all participating institutions to calculate radiation doses in a simple manner for consistency in delivered dose even though the accuracy was limited. Dose specification required use of a point-source approximation for ^{125}I source dosimetry with no corrections for dose anisotropy, plaque side or lip attenuation, lack of photon backscatter or fluorescence photons from the gold-alloy backing, or Silastic insert attenuation.[26] The COMS Radiation Committee members established these criteria at the time of trial formation based on the 1985 state-of-knowledge and availability of treatment planning capabilities in clinical practice.[24]

Since the COMS trials started, there have been several modifications to the recommended brachytherapy dosimetry formalism.[23,27–29] These modifications include new national primary air kerma strength calibration standards, and TG-43 dosimetry parameters for sources used in brachytherapy. In 1996, the original prescription dose of 100 Gy was revised to the equivalent 85 Gy based on the TG-43 formalism and dosimetry parameters published in 1995,[23] but the point source approximation and homogeneous water calculation continued to be used in the COMS protocol as rigidly specified in the COMS procedure manual.[24]

Recent updates of brachytherapy dosimetry guidelines, such as the 2004 and 2007 TG-43 Report Update and Supplement (TG-43U1 and TG-43U1S1) have addressed concerns regarding dose calculations to distances down to 1.0 mm (5 mm was the minimum distance in the 1995 TG-43 report) from low-energy brachytherapy seeds,[27,30] which is crucial for accurate calculation of doses to the tumor and critical ocular structures. In addition, the changes to new national primary air kerma strength calibration standards[28,29] were also adopted and incorporated in TG-43U1 and TG-43U1S1 for the recommendation of the revised dose rate constants and dosimetry formalisms.[27,30] These dosimetry data and formalisms (not available at the time of the COMS) are necessary for accurate calculation of eye tumor and critical ocular structure doses.[27,30–34] Similarly, functions have been examined to allow more accurate fitting of dosimetry parameters at short radial distances.[35] However, the AAPM recommendations in the TG-43U1 and TG-43U1S1 reports are limited to infinite homogeneous water medium and hence do not account for the effects of material heterogeneities such as the eye plaque and bony orbit which are of higher effective atomic number Z_{eff} than water.

The impact of these changes to calibration standards, dosimetry formalisms, and implant parameters has been examined by several investigators and evaluated by the AAPM for specific applications, e.g., low-energy prostate brachytherapy.[36,37] While specific clinical recommendations for choroidal melanoma were made by the ABS in 2003,[38] no societal guidance has been issued for the effects of new developments on modern eye-plaque dosimetry. Task Group 129 was formed to (a) review the dosimetry aspects of eye-plaque brachytherapy, (b) evaluate the impact of implementing the recommendations of TG-43U1 for the homogeneous assumption, (c) examine the heterogeneity effects on the dose distributions in the eye tumor and critical ocular structures, and (d) make recommendations for treatment planning and quality assurance (QA) for eye-plaque brachytherapy.

Many different possible designs of eye plaques, i.e., physical configurations, chemical compositions of components, and radionuclides, have been reported by various investigators.[2,25,39–57] These include COMS standard, notched and modified designs, ROPES, USC, IBt/Bebig (beta-emitters), Nag, and other custom made plaques. Among these designs, the COMS-plaques loaded with ^{125}I seeds are the most common. Besides ^{125}I seeds, COMS-plaques loaded with other low-energy radionuclide sources like ^{103}Pd and ^{131}Cs seeds have also been used for clinical treatment of ocular tumors.[3,4] Given the low-energy photons, ≤ 0.03 MeV, the heterogeneity effects due to the high Z_{eff} and physical densities of the gold-alloy backing and Silastic insert on the dose distributions are significant. While there are many potential plaque and seed combinations, the task group felt that it should focus on plaques of the standard COMS design for low-energy seeds due to their well-established use in the United States.

In this report, we present a detailed description of COMS-plaques in Sec. II. Review of eye-plaque dosimetry studies to 2011 and evaluation of the plaque heterogeneity effects on eye-plaque dose distributions are presented in Sec. III. Recommendations for eye-plaque treatment planning approaches and a quality management program (QMP) are presented in Sec. IV. The Appendix reviews the clinical aspects of eye-plaque brachytherapy of uveal melanoma and alternative radiation treatment modalities. These recommendations

have been reviewed and approved by the AAPM Brachytherapy Subcommittee, Therapy Physics Committee, and the Professional Council and by the ABS Board of Directors. This report is available on the AAPM website.[58] While certain commercial products are identified in this report, such identification does not imply recommendation nor endorsement by the AAPM or ABS, nor does it imply that the products are necessarily the best available for these purposes.

II. COMS PLAQUES

The standard COMS-plaque design (Figs. 1 and 2) consists of a gold-alloy backing (trade name Modulay)[59] and a Silastic (MDX4-4210 bio-medical grade elastomer; Dow Corning Corp., Midland, MI)[26] seed carrier insert. The COMS-plaques are available in 10 mm–22 mm diameters with 2 mm increments (Trachsel Dental Studio, Rochester, MN). Silastic inserts have grooves that reproducibly position brachytherapy seeds to provide approximately cylindrically symmetric dose distributions. The mass composition of the Modulay gold-alloy backing (density 15.8 g/cm^3) is 77%, 14%, 8%, and 1% of Au, Ag, Cu, and Pd, respectively.[59,60] The silicone rubber, Silastic, seed carrier insert is made of 39.9%, 28.9%, 24.9%, 6.3%, and 0.005% of Si, O, C, H, and Pt by weight, respectively,[26] with a physical density of 1.12 g/cm^3 and Z_{eff} = 11. Grooves on the convex side of the Silastic insert accommodate individual seeds, with the total number of seeds depending on plaque diameter. The Silastic layer between the bottom of the seed groove and the eye surface is 1 mm thick, serving as spacer material to avoid extreme dose "hot spots" in the scleral layer. The concave aspect of the Silastic insert has a radius of curvature of 12.3 mm designed to conform to the eye surface. The gold-alloy backing is in the form of a segment of spherical shell (0.5 mm thick and a 15.05 mm outer radius of curvature) terminated by a cylindrical segment, which is called the "lip." The lip provides radiation collimation for additional protection for normal structures around and in the eye.

Seed diagrams viewed from the concave side of the Silastic insert for seven different plaque sizes are shown in Fig. 1.[25] The seeds are generally arranged in polygon rings. The orientation of each seed is associated with an angle ϕ defined as the angle between the $+x_p$ axis and the projection on the x-y plane of the line passing through the seed center. For example, $\phi = 45^\circ$ and 135° for seeds # 3 and # 4, respectively, in the 10-mm plaque. The definition of angle ϕ indicating the orientation of each seed as shown in the diagram for the 10-mm plaque in Fig. 1 applies to all seeds in all the plaque sizes. The coordinates (in mm) of the seeds (centers and two ends) for standard plaques are listed in Table I in the eye-plaque coordinate system (x_p, y_p, z_p), where $z_p = 0$ (see Fig. 1) at the inner sclera point (1 mm interior of the outer sclera point) and the $+z_p$ axis points from the inner sclera into the eye. Seed coordinates are for the idealized positions for COMS-plaques. Values of ϕ angles for individual seeds are listed in the rightmost column of Table I. The seed center coordinates were based on the ring radius determined by Kline[61] and the angle ϕ for each seed for plaques 12 mm–20 mm in diameter. For 10 mm and 22 mm plaques, the ring radius values were determined using a digital caliper measurement, and angles ϕ for individual seeds were determined from scanned images of a set of Silastic inserts of these sizes. From the ring radius and angle ϕ, the seed center coordinates were calculated. The determination of the seed end coordinates was based on the seed center coordinates, the orientation of each seed, and the nominal seed physical length of 4.5 mm (seed physical length varies from 4.5 mm to 5.0 mm depending on seed model). The side view diagram of the 14 mm COMS-plaque in the plane (x_p-z_p plane) containing the plaque's central axis is shown in Fig. 2, with the seeds in idealized positions. Note that the seeds can move slightly away from the idealized positions in real patient cases. The users are advised to verify the coordinates of the loaded seeds in the plaque against the tabulated values in Table I at the time of plaque commissioning.

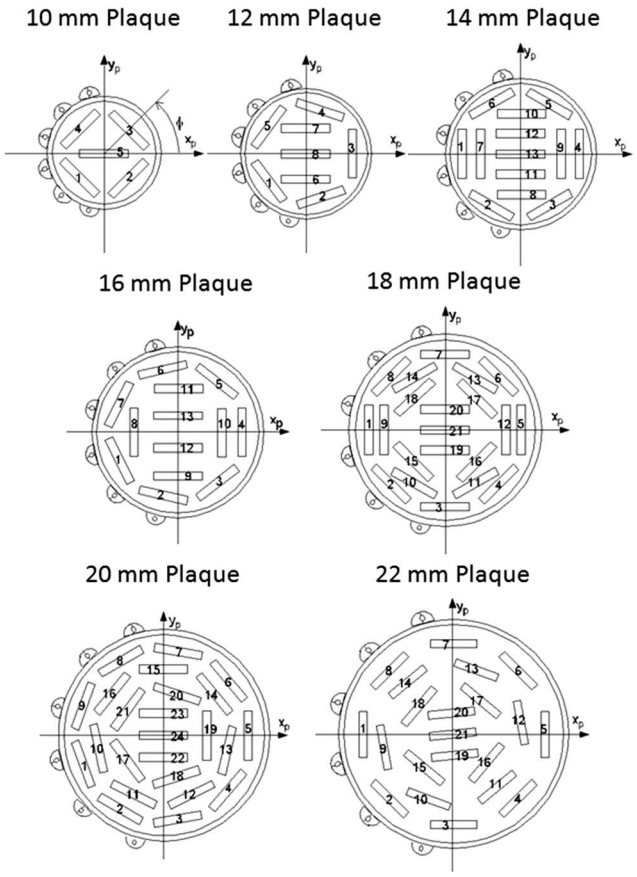

FIG. 1. Seed diagrams for 10 mm–22 mm COMS-plaques when viewed from the concave aspect of the Silastic insert. Rotational orientation of the Silastic seed carrier insert within the gold-alloy backing (relative to the suture eyelets) is arbitrary. The z_p axis (not shown) is pointing out of the image and toward the eye center. Note the angle ϕ defined as the angle between the $+x_p$ axis and the projection onto the x-y plane of the line passing through the seed center is shown in the diagram for the 10 mm plaque (upper left). This definition of angle ϕ applies to all plaque sizes.

III. DOSIMETRY STUDIES

Accurate eye-plaque dosimetry studies are challenging tasks due to steep dose gradient in the eye. The dosimetry studies for various designs of eye plaques (with different radionuclides and seed models) have

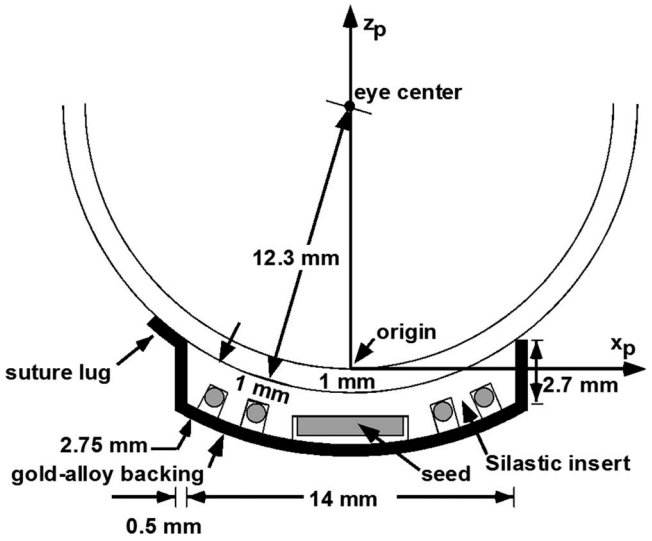

FIG. 2. Side view diagram of 14-mm COMS plaque, illustrating the gold-alloy backing and Silastic insert with seed grooves accommodating seeds (gray circles and rectangle) in idealized positions. The Silastic insert is 1 mm thick between the groove and the concave surface of the insert. The coordinate system origin is located at the inner sclera along the plaque central axis. The z_p-axis is pointing toward the eye center, the x_p-axis points away from the suture lug, and the y_p axis (not shown) points into the figure.

been reported, including measurements using thermoluminescent dosimeters (TLDs),[26,43,45,52,62–67] diodes,[45,68–70] radiographic film,[60,71] radiochromic film,[43,45,72–75] plastic scintillators,[76,77] polymer gel,[78] small ion chambers,[45] alanine,[45] and diamond,[45] as well as calculations using the TG-43 model and superposition,[52,79–81] Monte Carlo (MC) simulations,[26,44,49,53,59,82–86] and discrete-ordinates calculation method.[87,88] The dose distributions are highly sensitive to the plaque design, radionuclide selection and seed model, resulting in widely varying plaque heterogeneity effects. In view of the numerous designs of eye plaques and the sensitivity of the dose distributions to the plaque design, we focus this review on the most frequently used COMS-plaques as described in Sec. I. The task group evaluated all of the above-mentioned papers in developing its recommendations.

III.A. Literature review

In 1988, Wu and Krasin reported radiographic XV-film study results for 12-mm and 16-mm COMS-plaques, fully loaded with ^{125}I (model 6711) seeds.[60] The film was positioned in a central plane of the eye plaque. They reported relative doses normalized to 5 mm depth (on central axis) from the inner sclera, as presented in isodose curve plots in a central plane. They also demonstrated the collimating effect of the plaque lip on the dose distribution.

In the 1990s, Chiu-Tsao *et al.* and de la Zerda *et al.* reported on TLD measurements and MC simulations of the dose distributions in an eye phantom for single ^{125}I (model 6711) and ^{103}Pd (model 200) seeds at the center slot (# 24 as shown in Fig. 1) of a 20 mm COMS-plaque.[26,62,67] They observed central-axis dose reductions of about 10% and 16% at a depth of 10 mm for ^{125}I and ^{103}Pd, respectively, compared with doses in homogeneous water. The extent of dose reduction varied slowly with depth into the eye phantom. Off-axis dose reductions up to 30% were also reported. They attributed these reductions to the non-water-equivalence of the Silastic insert and lack of backscatter. Being 40% silicon by weight, Silastic has Z_{eff} greater than that of water ($Z_{eff} \sim 7.4$) and consequently attenuates low-energy photons more than water via the photoelectric effect. The study by de la Zerda *et al.* also included dose measurement at off-axis points extended to the penumbra region and beyond, to assess the penumbra characteristics in the central plane due to the collimating effect of the gold-alloy backing and lip.[62]

Knutsen *et al.*[70] performed diode measurements in water for 12-mm and 20-mm COMS-plaques loaded with ^{125}I seeds (model 6711 and 6702), reported relative doses along the central-axis and off-axis dose profiles, and compared these results with doses calculated using the Plaque Simulator (IBt-Bebig, Berlin, Germany) software.[70] Krintz *et al.* performed measurements using radiochromic (model MD55-2) film for 14-mm and 20-mm COMS plaques, fully loaded with ^{125}I seeds (model 6711) in a solid water phantom.[73] The film was positioned in a central plane of the plaque. They also reported relative doses along the central-axis and off-axis profiles, which were compared with Plaque Simulator software calculated dose distributions using a line source approximation and a constant correction factor of 0.9 in version 4. Measured off-axis doses were lower than those calculated by an average of 15% near the plaque periphery, demonstrating that the use of a constant correction factor was inadequate to account for the extra attenuation resulting from radiation traveling a longer path (greater than 1 mm) tangentially through Silastic.

The COMS medium tumor trial dosimetry was reanalyzed by Krintz *et al.* in 2003 to investigate the impact of dose anisotropy, the line-source approximation for the geometry function, radiation collimation by the gold-alloy backing, and Silastic seed carrier insert attenuation using an early version of Plaque Simulator software.[73,74] The reanalysis used a constant Silastic transmission factor of 0.9 (10% reduction) based on Chiu-Tsao *et al.*[26] and a gold transmission factor of zero. They determined that corrected dose calculations resulted in a significant reduction, between 7% and 21%, compared to COMS-calculated values for structures of interest within the eye. The authors concluded that future eye-plaque dosimetry should be "performed using the most up-to-date parameters available." However, even the most recent 2D dose calculation algorithm in the 2004 and 2007 AAPM TG-43 reports will over-estimate dose due to the inherent assumption of an infinite homogeneous water medium used to obtain seed dosimetry parameter data.

In 2008, Rivard *et al.* reported dosimetry data for standard COMS-plaques with diameters between 10 mm and 22 mm, and for specific ^{125}I (model 6711), ^{103}Pd (model 200), and ^{131}Cs (model CS-1 Rev2) seeds, based on superposition of dose contributions from individual seeds following the TG-43 formalism in an infinite homogeneous water medium using the Pinnacle treatment planning system.[89] Treatment times to deliver appropriate doses were provided. Although

TABLE I. Coordinates (millimeters) of seeds for the 10 mm–22 mm diameter COMS standard eye plaques. The seed physical length was set to 4.5 mm. Physical positioning of the seed # assignment is shown in Fig. 1. The COMS reference coordinate system origin at ($x_p = 0$, $y_p = 0$, $z_p = 0$) is defined at the inner sclera along the plaque's central axis. The angle ϕ is the angle between the $+x_p$ axis and the projection on the x-y plane of the line from the origin to the seed center. As an example, the definition of the angle ϕ is shown in the diagram for 10 mm plaque in Fig. 1. In this example, $\phi = 45^\circ$ for seed # 3.

		Seed center coordinates			Seed end coordinates						Angle
	Seed #	x_{pc}	y_{pc}	z_{pc}	x_{p1}	y_{p1}	z_{p1}	x_{p2}	y_{p2}	z_{p2}	ϕ (°)
10 mm plaque	1	−2.30	−2.30	−2.01	−3.89	−0.71	−2.01	−0.71	−3.89	−2.01	225
	2	2.30	−2.30	−2.01	0.71	−3.89	−2.01	3.89	−0.71	−2.01	315
	3	2.30	2.30	−2.01	3.89	0.71	−2.01	0.71	3.89	−2.01	45
	4	−2.30	2.30	−2.01	−0.71	3.89	−2.01	−3.89	0.71	−2.01	135
	5	0.00	0.00	−2.40	2.25	0.00	−2.40	−2.25	0.00	−2.40	90
12 mm plaque	1	−3.72	−2.70	−1.60	−5.04	−0.88	−1.60	−2.40	−4.52	−1.60	216
	2	1.42	−4.37	−1.60	−0.72	−5.07	−1.60	3.56	−3.68	−1.60	288
	3	4.60	0.00	−1.60	4.60	−2.25	−1.60	4.60	2.25	−1.60	0
	4	1.42	4.37	−1.60	3.56	3.68	−1.60	−0.72	5.07	−1.60	72
	5	−3.72	2.70	−1.60	−2.40	4.52	−1.60	−5.04	0.88	−1.60	144
	6	0.00	−2.70	−2.13	−2.25	−2.70	−2.13	2.25	−2.70	−2.13	270
	7	0.00	2.70	−2.13	2.25	2.70	−2.13	−2.25	2.70	−2.13	90
	8	0.00	0.00	−2.40	2.25	0.00	−2.40	−2.25	0.00	−2.40	90
14 mm plaque	1	−5.90	0.00	−1.06	−5.90	2.25	−1.06	−5.90	−2.25	−1.06	180
	2	−2.95	−5.11	−1.06	−4.90	−3.98	−1.06	−1.00	−6.23	−1.06	240
	3	2.95	−5.11	−1.06	1.00	−6.23	−1.06	4.90	−3.98	−1.06	300
	4	5.90	0.00	−1.06	5.90	−2.25	−1.06	5.90	2.25	−1.06	0
	5	2.95	5.11	−1.06	4.90	3.98	−1.06	1.00	6.23	−1.06	60
	6	−2.95	5.11	−1.06	−1.00	6.23	−1.06	−4.90	3.98	−1.06	120
	7	−4.10	0.00	−1.77	−4.10	2.25	−1.77	−4.10	−2.25	−1.77	180
	8	0.00	−4.10	−1.77	−2.25	−4.10	−1.77	2.25	−4.10	−1.77	270
	9	4.10	0.00	−1.77	4.10	−2.25	−1.77	4.10	2.25	−1.77	0
	10	0.00	4.10	−1.77	2.25	4.10	−1.77	−2.25	4.10	−1.77	90
	11	0.00	−2.10	−2.24	−2.25	−2.10	−2.24	2.25	−2.10	−2.24	270
	12	0.00	2.10	−2.24	2.25	2.10	−2.24	−2.25	2.10	−2.24	90
	13	0.00	0.00	−2.40	2.25	0.00	−2.40	−2.25	0.00	−2.40	90
16 mm plaque	1	−5.68	−2.73	−0.87	−6.65	−0.71	−0.87	−4.70	−4.76	−0.87	206
	2	−1.40	−6.14	−0.87	−3.60	−5.64	−0.87	0.79	−6.64	−0.87	257
	3	3.93	−4.93	−0.87	2.17	−6.33	−0.87	5.69	−3.52	−0.87	309
	4	6.30	0.00	−0.87	6.30	−2.25	−0.87	6.30	2.25	−0.87	0
	5	3.93	4.93	−0.87	5.69	3.52	−0.87	2.17	6.33	−0.87	51
	6	−1.40	6.14	−0.87	0.79	6.64	−0.87	−3.60	5.64	−0.87	103
	7	−5.68	2.73	−0.87	−4.70	4.76	−0.87	−6.65	0.71	−0.87	154
	8	−4.50	0.00	−1.64	−4.50	2.25	−1.64	−4.50	−2.25	−1.64	180
	9	0.00	−4.50	−1.64	−2.25	−4.50	−1.64	2.25	−4.50	−1.64	270
	10	4.50	0.00	−1.64	4.50	−2.25	−1.64	4.50	2.25	−1.64	0
	11	0.00	4.50	−1.64	2.25	4.50	−1.64	−2.25	4.50	−1.64	90
	12	0.00	−1.80	−2.28	−2.25	−1.80	−2.28	2.25	−1.80	−2.28	270
	13	0.00	1.80	−2.28	2.25	1.80	−2.28	−2.25	1.80	−2.28	90
18 mm plaque	1	−7.70	0.00	−0.03	−7.70	2.25	−0.03	−7.70	−2.25	−0.03	180
	2	−5.44	−5.44	−0.03	−7.04	−3.85	−0.03	−3.85	−7.04	−0.03	225
	3	0.00	−7.70	−0.03	−2.25	−7.70	−0.03	2.25	−7.70	−0.03	270
	4	5.44	−5.44	−0.03	3.85	−7.04	−0.03	7.04	−3.85	−0.03	315
	5	7.70	0.00	−0.03	7.70	−2.25	−0.03	7.70	2.25	−0.03	0
	6	5.44	5.44	−0.03	7.04	3.85	−0.03	3.85	7.04	−0.03	45
	7	0.00	7.70	−0.03	2.25	7.70	−0.03	−2.25	7.70	−0.03	90
	8	−5.44	5.44	−0.03	−3.85	7.04	−0.03	−7.04	3.85	−0.03	135
	9	−6.20	0.00	−0.92	−6.20	2.25	−0.92	−6.20	−2.25	−0.92	180
	10	−3.10	−5.37	−0.92	−5.05	−4.24	−0.92	−1.15	−6.49	−0.92	240
	11	3.10	−5.37	−0.92	1.15	−6.49	−0.92	5.05	−4.24	−0.92	300
	12	6.20	0.00	−0.92	6.20	−2.25	−0.92	6.20	2.25	−0.92	0
	13	3.10	5.37	−0.92	5.05	4.24	−0.92	1.15	6.49	−0.92	60

TABLE I. *(Continued).*

		Seed center coordinates			Seed end coordinates						Angle
	Seed #	x_{pc}	y_{pc}	z_{pc}	x_{p1}	y_{p1}	z_{p1}	x_{p2}	y_{p2}	z_{p2}	ϕ (°)
	14	−3.10	5.37	−0.92	−1.15	6.49	−0.92	−5.05	4.24	−0.92	120
	15	−3.18	−3.18	−1.64	−4.77	−1.59	−1.64	−1.59	−4.77	−1.64	225
	16	3.18	−3.18	−1.64	1.59	−4.77	−1.64	4.77	−1.59	−1.64	315
	17	3.18	3.18	−1.64	4.77	1.59	−1.64	1.59	4.77	−1.64	45
	18	−3.18	3.18	−1.64	−1.59	4.77	−1.64	−4.77	1.59	−1.64	135
	19	0.00	−2.00	−2.25	−2.25	−2.00	−2.25	2.25	−2.00	−2.25	270
	20	0.00	2.00	−2.25	2.25	2.00	−2.25	−2.25	2.00	−2.25	90
	21	0.00	0.00	−2.40	2.25	0.00	−2.40	−2.25	0.00	−2.40	90
20 mm plaque	1	−8.08	−2.94	0.64	−8.85	−0.83	0.64	−7.31	−5.06	0.64	200
	2	−4.30	−7.45	0.64	−6.25	−6.32	0.64	−2.35	−8.57	0.64	240
	3	1.49	−8.47	0.64	−0.72	−8.86	0.64	3.71	−8.08	0.64	280
	4	6.59	−5.53	0.64	5.14	−7.25	0.64	8.03	−3.80	0.64	320
	5	8.60	0.00	0.64	8.60	−2.25	0.64	8.60	2.25	0.64	0
	6	6.59	5.53	0.64	8.03	3.80	0.64	5.14	7.25	0.64	40
	7	1.49	8.47	0.64	3.71	8.08	0.64	−0.72	8.86	0.64	80
	8	−4.30	7.45	0.64	−2.35	8.57	0.64	−6.25	6.32	0.64	120
	9	−8.08	2.94	0.64	−7.31	5.06	0.64	−8.85	0.83	0.64	160
	10	−6.53	−1.49	−0.65	−7.03	0.70	−0.65	−6.03	−3.68	−0.65	193
	11	−2.91	−6.04	−0.65	−4.93	−5.06	−0.65	−0.88	−7.01	−0.65	244
	12	2.91	−6.04	−0.65	0.88	−7.01	−0.65	4.93	−5.06	−0.65	296
	13	6.53	−1.49	−0.65	6.03	−3.68	−0.65	7.03	0.70	−0.65	347
	14	5.24	4.18	−0.65	6.64	2.42	−0.65	3.84	5.94	−0.65	39
	15	0.00	6.70	−0.65	2.25	6.70	−0.65	−2.25	6.70	−0.65	90
	16	−5.24	4.18	−0.65	−3.84	5.94	−0.65	−6.64	2.42	−0.65	141
	17	−3.80	−2.76	−1.57	−5.12	−0.94	−1.57	−2.48	−4.58	−1.57	216
	18	1.45	−4.47	−1.57	−0.69	−5.17	−1.57	3.59	−3.77	−1.57	288
	19	4.70	0.00	−1.57	4.70	−2.25	−1.57	4.70	2.25	−1.57	0
	20	1.45	4.47	−1.57	3.59	3.77	−1.57	−0.69	5.17	−1.57	72
	21	−3.80	2.76	−1.57	−2.48	4.58	−1.57	−5.12	0.94	−1.57	144
	22	0.00	−2.25	−2.21	−2.25	−2.25	−2.21	2.25	−2.25	−2.21	270
	23	0.00	2.25	−2.21	2.25	2.25	−2.21	−2.25	2.25	−2.21	90
	24	0.00	0.00	−2.40	2.25	0.00	−2.40	−2.25	0.00	−2.40	90
22 mm plaque	1	−9.20	0.00	1.15	−9.20	2.25	1.15	−9.20	−2.25	1.15	180
	2	−6.51	−6.51	1.15	−8.10	−4.91	1.15	−4.91	−8.10	1.15	225
	3	0.00	−9.20	1.15	−2.25	−9.20	1.15	2.25	−9.20	1.15	270
	4	6.51	−6.51	1.15	4.91	−8.10	1.15	8.10	−4.91	1.15	315
	5	9.20	0.00	1.15	9.20	−2.25	1.15	9.20	2.25	1.15	0
	6	6.51	6.51	1.15	8.10	4.91	1.15	4.91	8.10	1.15	45
	7	0.00	9.20	1.15	2.25	9.20	1.15	−2.25	9.20	1.15	90
	8	−6.51	6.51	1.15	−4.91	8.10	1.15	−8.10	4.91	1.15	135
	9	−7.19	−1.27	−0.29	−7.58	0.95	−0.29	−6.80	−3.48	−0.29	190
	10	−2.50	−6.86	−0.29	−4.61	−6.09	−0.29	−0.38	−7.63	−0.29	250
	11	4.69	−5.59	−0.29	2.97	−7.04	−0.29	6.42	−4.15	−0.29	310
	12	7.19	1.27	−0.29	7.58	−0.95	−0.29	6.80	3.48	−0.29	10
	13	2.50	6.86	−0.29	4.61	6.09	−0.29	0.38	7.63	−0.29	70
	14	−4.69	5.59	−0.29	−2.97	7.04	−0.29	−6.42	4.15	−0.29	130
	15	−3.09	−3.68	−1.53	−4.81	−2.23	−1.53	−1.36	−5.12	−1.53	230
	16	3.68	−3.09	−1.53	2.23	−4.81	−1.53	5.12	−1.36	−1.53	320
	17	3.09	3.68	−1.53	4.81	2.23	−1.53	1.36	5.12	−1.53	50
	18	−3.68	3.09	−1.53	−2.23	4.81	−1.53	−5.12	1.36	−1.53	140
	19	0.20	−2.24	−2.21	−2.05	−2.44	−2.21	2.44	−2.05	−2.21	275
	20	−0.20	2.24	−2.21	2.05	2.44	−2.21	−2.44	2.05	−2.21	95
	21	0.00	0.00	−2.40	2.24	0.20	−2.40	−2.24	−0.20	−2.40	95

the plaque heterogeneity effect was not accounted for in this study, the comparison of dose distributions and dose-volume histograms for the three radionuclides provided information concerning the choice of radionuclide and implant time based on plaque size and tumor apex height. In this paper, the correction for the NIST 1999 S_K update was incorrectly implemented a second time when establishing the acceptable dose-rate criterion using the methods of the 2003 ABS guidance publication.

In 2008, Melhus and Rivard reported results of MC simulations using MCNP5 that were performed to estimate brachytherapy dose distributions for COMS eye plaques.[82] Specific brachytherapy source models containing ^{125}I (model 6711), ^{103}Pd (model 200), and ^{131}Cs (model CS-1 Rev2) were distributed into 10 mm–22 mm diameter COMS eye plaques. Transport media used in the MC simulations were both heterogeneous (Hetero), including Silastic and gold-alloy backing, and homogeneous (Homo) liquid water environments. Homogeneous central-axis dose distributions agreed to within 2% to Pinnacle calculated values based on the TG-43 approach.[90] For heterogeneous simulations, notable radiation dose attenuation was observed with reductions at 5 mm depth of 11%, 19%, and 9% for ^{125}I, ^{103}Pd, and ^{131}Cs, respectively. A depth-dependent central-axis dose correction factor (referred to as Hetero/Homo ratio) was derived to correct homogenous dose calculations at depths up to 10 mm from the inner sclera for COMS-plaque component heterogeneity effects with plaques fully loaded with seeds. The ratio decreased slowly with increasing depth into the eye. They also performed MC simulations for single seeds at the center of a 20 mm COMS plaque in homogeneous water medium for comparison with a fully loaded plaque.

Also in 2008, Thomson *et al.* reported results of a MC investigation of eye-plaque brachytherapy dosimetry using BrachyDose, an EGSnrc-based radiation transport code, to simulate 3D dose distributions in the eye from specific ^{125}I (model 6711) and ^{103}Pd (model 200) sources in standard COMS-plaques.[59] Homogenous water medium was generally assessed, and implications of replacing water with eye tissues were examined. Dosimetric influence of the gold-alloy backing was investigated, and found to be sensitive to the backing composition. For a fully loaded plaque with gold-alloy backing and Silastic insert, the dose decrease relative to homogeneous water was 13% for ^{125}I and 20% for ^{103}Pd at a distance of 5 mm from the inner sclera along the plaque's central axis. For COMS-plaques, inter-seed attenuation was observed to be a 2% effect. Dose reduction near the air-tissue interface (in front of cornea) was up to 10% as compared to an infinite homogeneous water medium, but the effect was small at most points-of-interest (POIs) within the eye. Similarly, orbital bones were shown to decrease doses in the eye region by up to 5% and 3.5% for ^{125}I and ^{103}Pd, respectively, depending on the plaque location on the eyeball. Replacing water as the transport medium with eye tissue and surrounding air resulted in dosimetric differences of up to 8%.[59] For the same prescription dose, ^{103}Pd generally delivered a lower dose than ^{125}I to normal or critical structures. Furthermore, the authors observed that BrachyDose was sufficiently fast to allow full MC dose calculations for routine clinical treatment planning. In addition to fully loaded plaques, they performed MC simulations for a single seed at the center of a 12 mm or 20 mm COMS plaque in a homogeneous water medium. They determined the Hetero/Homo ratio at depths $\leq$ 23 mm for both single seed and fully loaded plaques. It was found that the values of the Hetero/Homo ratio for a fully loaded 16 mm COMS plaque differed by up to 2% on the central axis and by up to nearly 6% at other POIs. For a single seed in 12-mm and 20-mm plaques, the values of the Hetero/Homo ratio were within 1%, hence insensitive to the plaque size.

There is good agreement between the results of BrachyDose and MCNP5 simulations for ^{125}I (model 6711) and ^{103}Pd (model 200) seeds in the COMS-plaques, with the BrachyDose simulation covering a larger region around the eye. The Hetero/Homo ratio for single seed ^{125}I (model 6711) and ^{103}Pd (model 200) at the center of a 20 mm COMS plaque obtained from these two MC codes was compared with the TLD data for the same seed model by de la Zerda *et al.*[62] and Chiu-Tsao *et al.*[67] Agreement within the uncertainties of both the TLD data ($\pm$ 5%–10%) and MC results (<0.4% statistical uncertainty only) was found. Thus, the TLD data corroborate the MC simulation results of the dose reduction by COMS-plaque.

In 2010, Thomson and Rogers reported on the sensitivity of dose distributions for eye-plaque brachytherapy as a function of seed model.[83] Using BrachyDose, they calculated dose distributions for six ^{103}Pd and ^{125}I seed models identified to have sufficient air kerma strength for eye-plaque therapy and compared these to previously obtained results.[59] Differences in dose reduction relative to homogeneous water assumption (based on TG-43 approach) varied slightly with seed model, with variations generally of order 2%. For the same prescription dose, absolute doses at POIs vary by up to 8% with seed model (see Tables III–V in Thomson and Rogers[83] for doses at POIs for different seed models). In general, for the same prescription dose at the prescription point, doses at selected POIs were lower with ^{103}Pd seed models than with ^{125}I seeds. This study also demonstrated the large errors incurred using the TG-43 approach (homogeneous water assumption) to calculate doses to critical ocular structures, particularly to points off the plaque's central axis with dose differences of up to 90% observed.[59]

In 2010, Thomson *et al.* reported on MC results, also using BrachyDose code, for a modified 22 mm COMS plaque with a 10 mm diameter circular cutout at the plaque center designed for treatment of iris melanomas.[53] The plaque was loaded with ^{125}I (model 6711) or ^{103}Pd (model 200) seeds. Doses at POIs differed by up to 70% from those calculated using the superposition method based on the TG-43 approach, indicating the importance of accounting for attenuation and lack of scatter by the plaque.

Zhang *et al.* reported on MC simulations for a 16 mm COMS plaque without the Silastic insert.[86] The plaque was fully loaded with ^{125}I seeds (IsoAid model IAI-125A) or ^{131}Cs seeds (IsoRay model CS-1 Rev2) in a water equivalent insert. MCNPX code was used for the calculation. They compared the heterogeneity effects due to gold and gold-alloy plaques

on the central-axis doses and dose-volume histograms for ^{125}I and ^{131}Cs sources, and found dose reductions of 7% and 4% for gold and gold-alloy backings at a depth of 6 mm compared to the homogeneous water conditions.

Acar[75] reported radiochromic EBT film measurement of dose distributions for COMS-plaques with diameters of 14 mm, 16 mm, 18 mm, and 20 mm fully loaded with ^{125}I seeds (IBt-Bebig model I25.S16). EBT film was positioned in a central plane of the plaque in a polystyrene eye phantom. In addition, a film was also positioned at 5 mm or 12 mm depth normal to the plaque central axis. The relative central-axis doses normalized to the 5 mm depth as well as relative off-axis dose profiles were reported. The EBT film data were compared with the calculated relative doses using Plaque Simulator (version 4) and were lower by no more than 15%.

In 2011, Rivard *et al.* compared three clinical brachytherapy TPS and two MC codes to investigate dosimetric differences for brachytherapy of intraocular tumors using specific ^{125}I (model 6711) or ^{103}Pd (model 200) sources in a 16 mm COMS plaque.[90] The authors evaluated the impact of heterogeneity-enabled MC estimations on the administered dose. TPS used in the comparison were BrachyVision v6.1 and v8.1, Plaque Simulator v5.3.9, and Pinnacle v8.0dp1, all of which use the superposition of single seed doses following the AAPM TG-43U1 point-source (1D) or line-source (2D) formalisms in water. Using modified 2D dose calculations accounting for the plaque heterogeneity, the Plaque Simulator software can also incorporate correction factors for individual seeds due to gold-alloy backing and Silastic insert. MCNP5 v1.40 and BrachyDose/EGSnrc MC codes were used for comparison to the TG-43 techniques. Three types of calculations were performed: (1) point source approximation (1D TG-43U1 formalism) in homogeneous water medium (for the TPS only), (2) line source approximation (TPS with 2D TG-43U1 formalism and MC codes) in homogeneous water medium, and (3) plaque heterogeneity-corrected line sources (Plaque Simulator with modified 2D calculation and MC codes). Comparisons between the five methods were made along the plaque central axis and at specified off-axis points representing normal anatomic structures within a standardized eye model. For TG-43 calculations in a homogeneous water medium, agreement within 2% was observed between the 1D and 2D formalisms when comparing TPS and MC codes. For the heterogeneous dose calculations, the results from MC codes and modified 2D calculation in Plaque Simulator agreed within 2% at most points along the central axis. Dose differences for plaque heterogeneity-corrected calculations differed by up to 37% on the central axis in comparison to a homogeneous water medium. Rivard *et al.*[90] determined that a prescription dose of 85 Gy (based on homogeneous water assumption) at 5 mm depth actually delivers 76 Gy and 67 Gy for specific ^{125}I (model 6711) and ^{103}Pd (model 200) sources, respectively, after accounting for COMS-plaque heterogeneities. For off-axis anatomic structures, dose differences between homogeneous water and heterogeneous medium cases approached a factor of 10.

III.B. Plaque Simulator TPS

After consideration of the COMS dosimetry correction factors examined by Krintz *et al.*,[74] Astrahan included additional correction factors into a later version (version 5) of Plaque Simulator software.[79] Though this is the only currently available software specific to eye-plaque treatment planning,[79] it is not approved by the U.S. Food and Drug Administration (FDA) nor has it received the Conformité Européenne (CE) mark as of this writing. Plaque Simulator is based on superposition of dose contributions from individual seeds following the TG-43 formalism. The software incorporates additional features that model three-dimensionally the gold-alloy backing and ray-trace the path of primary radiation between the calculation point and a linear radiation source. This enables the software to account for collimation of primary radiation emitted from the radioactive seeds by the gold-alloy backing. The software also incorporates a scatter and attenuation correction factor specific to COMS plaques that is estimated from the primary path length in the Silastic seed carrier insert and is dependent on the distance between the source and calculation point. In addition, there is a fluorescence backscatter correction factor for the USC style plaques[91] in which the seeds are glued directly into individually collimating slots embedded in the gold backing. Compared with homogeneous water, the dose-modifying effects of the gold-alloy backing and Silastic were greatest near the plaque surface and immediately adjacent to the plaque, while being least near the center of the eye. The dose distribution calculated using Plaque Simulator surrounding a single ^{125}I seed (model 6711) centered in a 20-mm COMS-plaque was consistent with previously published studies using TLD measurement and MC calculation.[26,62] For fully loaded 12-mm and 20-mm plaques, Astrahan concluded that the calculated dose to critical ocular structures ranged from 16% to 50% less than that reported using the standard COMS dose calculation protocol. The 50% reduction occurred at a point of interest in the penumbra region of a 12 mm plaque, illustrating the collimating effect of the gold-alloy backing and lip accounted for in the Plaque Simulator calculation. Also in 2005, Astrahan *et al.* described the dosimetric consideration of a modified COMS-plaque with a reusable gold "seed-guide" insert replacing the Silastic insert.[50] The seed locations in such a "seed guide" insert are slightly different from those of the Silastic insert. Hence, the dose distribution is different from that for a COMS-plaque with Silastic insert. The effect on doses due to the air space between the seeds and the eye surface was also estimated.

Review of current clinical practice indicates several brachytherapy software programs employed for plaque dose calculations. Though many of these programs have been approved for general brachytherapy applications, Plaque Simulator is the only one specifically written for ophthalmic plaque dosimetry. It is widely used and commercially available (IBt-Bebig, Germany), and has many image-based features not available in custom Excel spreadsheets developed institutionally for plaque dose calculations and checks. Until Plaque

Simulator receives approval by the U.S. Food and Drug Administration, the AAPM and ABS do not recommend its clinical use as a primary dose calculation tool.

III.C. TG-43 hybrid treatment planning

In 2009, Rivard *et al.* developed an approach to using a conventional brachytherapy TPS for treatment planning of complex, MC-based brachytherapy dose distributions that include material heterogeneities.[92] Each COMS eye plaque fully loaded with radioactive seeds was modeled as a virtual source. The longitudinal axis (z-axis) of the virtual source coincided with the plaque central axis. The 2D anisotropy function in the cylindrical coordinate system and the radial dose function for the virtual source were obtained from the MC-derived dose distributions and entered into the Pinnacle TPS. They demonstrated that this approach could accurately reproduce MC-derived heterogeneous-corrected dose distributions for plaques fully loaded with ^{125}I, ^{103}Pd, or ^{131}Cs seeds. Drawbacks of this technique are (a) the volume averaging about the plaque axis of symmetry, and (b) the number of dosimetric parameter values (exceeding 30 000 for each combination of radionuclide and plaque size) needed for TPS entry.

IV. RECOMMENDATIONS

In the interim before brachytherapy TPS allowing heterogeneity-corrected dose calculations become FDA approved or receive CE mark and are commercially available, the AAPM and ABS recommend a dual approach (i.e., separate homogeneous and heterogeneous dose calculations) for eye-plaque treatment planning as outlined in Secs. IV.A and IV.B. Guidance on seed dosimetry parameters, image-guided brachytherapy, and the quality management program are also provided in Subsections IV.A–IV.E.

IV.A. Homogeneous dose calculation formalisms

The AAPM TG-43 1D formalism was used in the original COMS protocol for central-axis dose calculations with the 1D anisotropy function $\phi_{an}(r)$ set equal to unity. In comparison to the 2D formalism, this approximation produces nearly identical central-axis dose results because COMS plaque source positioning aligns the transverse planes of every source with the plaque central-axis. However, dose differences >5% between the 1D and 2D formalisms exist away from the plaque central-axis. Because source orientations are known and affixed by the Silastic insert, the AAPM and ABS recommend abandonment of the 1D formalism dose calculation method and use of the 2D brachytherapy dosimetry formalism of the AAPM TG-43U1 report. Care should be taken to ensure that the line-source geometry function is used with the radial dose function $g_L(r)$ and 2D anisotropy function $F(r, \theta)$.[27] The clinical medical physicist (or Qualified Medical Physicist depending on the regulatory environment) should discuss changing from the 1D to the 2D formalism with their radiation oncologist colleague(s) prescribing eye plaque brachytherapy.

IV.B. Heterogeneous dose calculation formalisms

In light of the clinically significant radiation collimation by high-Z plaque components, the clinical medical physicist should prepare for a transition to more accurate dose calculations. Based on the magnitude and clinical significance of the plaque heterogeneity effects mentioned in Sec. III, the AAPM and ABS recommend that dose calculations be performed in both homogeneous water (i.e., TG-43 dosimetry formalism) and accounting for plaque material heterogeneities. The AAPM and ABS recognize that the most accurate method to calculate eye-plaque brachytherapy dose distributions is a verified MC code that accounts for material heterogeneities of the eye plaque and patient. However, there currently are no MC-based TPS having FDA approval or CE mark. Accurate eye-plaque dosimetry may also be obtained with conventional brachytherapy TPS based on the TG-43 hybrid technique,[92,93] or using the superposition of single-source dose distributions with appropriate semianalytic corrections for plaque material heterogeneities such as performed by Plaque Simulator software. However, until brachytherapy MC-based TPS or the Plaque Simulator software obtain FDA approval or CE mark, clinical practitioners may be limited to the TG-43 hybrid technique or conventional TG-43-based dose calculations in homogeneous water medium.

In anticipation of brachytherapy TPS allowing heterogeneous dose calculations, e.g., semianalytic path-length correction,[79] MC,[59,82,83] collapsed cone,[94,95] discrete ordinates,[87,88] or other approaches,[92] the AAPM and ABS recommend performing a parallel dose calculation or estimation to include the effects of plaque material heterogeneities when these brachytherapy TPS become available. At a minimum, heterogeneity-corrected dose to the prescription point should be obtained, but preferably a 2D dose distribution. To aid the treatment planning decision making process, a table of central-axis dose values for Homo and Hetero cases for fully loaded plaques is presented based on the MC results by Thomson *et al.*[59] Table II displays the central-axis dose values of the Homo and Hetero cases for all seven COMS-plaque sizes, with the Homo dose normalized to 85 Gy at a depth of 5 mm for a given plaque size. Table II facilitates estimations of the administered dose with the plaque heterogeneity accounted for corresponding to calculated dose with homogeneous assumption, using the same product of the air kerma strength and effective treatment time, correcting for decay during the elapsed treatment time. When the prescription point is the tumor apex at a depth different from 5 mm, the tabulated Homo value at that prescription depth should be renormalized to the prescription dose, and all the other values (Hetero and Homo) for the same plaque size in the same table should be rescaled accordingly. For example, when the prescription dose is 85 Gy (with homogeneous water assumption) at the prescription depth of 7 mm for a 16 mm plaque loaded with ^{125}I (model 6711) seeds, the dose values as listed

TABLE II. Central-axis dose values (in Gy) of the Homo and Hetero cases for all seven COMS plaque sizes (10 mm–22 mm), with the Homo dose normalized to 85 Gy at a depth of 5 mm for a given plaque size. Data are for model 6711 and model 200 seeds for ^{125}I and ^{103}Pd, respectively, from simulations with BrachyDose (Ref. 54).

	Homo							Hetero						
Depth (mm)	10	12	14	16	18	20	22	10	12	14	16	18	20	22
^{125}I (6711)														
0	445	363	320	262	252	231	236	395	317	278	223	215	196	202
1	295	255	232	204	192	181	180	263	226	204	177	166	155	155
2	205	187	175	162	153	147	145	184	166	155	142	134	127	126
3	149	141	135	130	125	121	120	133	125	120	114	109	106	104
4	111	108	107	104	103	101	101	98.5	96.0	93.9	92.0	89.8	88.4	87.7
5	85.0	85.0	85.0	85.0	85.0	85.0	85.0	75.0	74.9	74.8	74.6	74.4	74.4	74.1
6	66.9	67.8	68.7	69.7	70.8	71.7	72.3	58.5	59.4	60.2	60.9	61.8	62.5	62.8
7	53.5	54.9	56.3	57.6	59.4	60.8	61.6	46.5	47.8	49.0	50.1	51.6	52.9	53.5
8	43.5	45.0	46.5	48.0	50.1	51.8	52.9	37.6	38.9	40.3	41.7	43.4	44.8	45.7
9	35.9	37.3	38.9	40.4	42.5	44.1	45.5	30.8	32.2	33.5	34.9	36.6	38.1	39.2
10	30.0	31.3	32.9	34.3	36.3	38.0	39.4	25.6	26.9	28.1	29.4	31.2	32.6	33.7
11	25.3	26.7	28.0	29.2	31.2	32.8	34.0	21.5	22.6	23.9	25.0	26.6	28.0	29.1
12	21.6	22.7	24.0	25.1	26.9	28.5	29.6	18.2	19.2	20.4	21.3	22.9	24.2	25.3
13	18.5	19.5	20.7	21.7	23.4	24.8	25.9	15.6	16.5	17.4	18.4	19.8	21.0	21.9
14	16.1	16.9	17.9	18.9	20.5	21.8	22.7	13.4	14.2	15.1	16.0	17.2	18.3	19.2
15	14.0	14.8	15.7	16.6	17.9	19.1	20.0	11.6	12.3	13.1	13.9	15.0	16.0	16.7
16	12.2	13.0	13.8	14.5	15.8	16.9	17.7	10.1	10.8	11.4	12.2	13.1	14.1	14.8
17	10.7	11.4	12.2	12.8	14.0	14.9	15.7	8.88	9.43	10.0	10.7	11.6	12.4	13.0
18	9.51	10.1	10.8	11.4	12.4	13.2	14.0	7.85	8.33	8.90	9.47	10.2	11.0	11.5
19	8.46	9.00	9.54	10.1	11.0	11.9	12.4	6.94	7.37	7.88	8.36	9.06	9.72	10.3
20	7.56	8.03	8.52	9.01	9.85	10.6	11.1	6.17	6.55	7.02	7.43	8.07	8.65	9.12
21	6.74	7.21	7.64	8.09	8.87	9.44	9.98	5.52	5.85	6.24	6.67	7.25	7.75	8.11
22	6.04	6.43	6.85	7.27	7.97	8.52	9.00	4.94	5.24	5.59	5.95	6.49	6.90	7.26
23	5.45	5.77	6.18	6.56	7.18	7.68	8.16	4.40	4.70	5.00	5.36	5.82	6.26	6.59
^{103}Pd (200)														
0	483	396	350	288	276	253	258	376	302	263	211	203	185	191
1	324	281	255	224	211	197	197	260	222	199	172	162	151	151
2	224	203	190	175	166	158	156	181	163	151	137	130	123	122
3	158	150	143	137	132	128	126	129	121	115	109	105	101	100
4	115	112	110	108	106	104	103	93.4	90.8	88.6	86.5	84.6	83.0	82.3
5	85.0	85.0	85.0	85.0	85.0	85.0	85.0	69.2	69.0	68.8	68.5	68.4	68.1	67.9
6	64.5	65.6	66.5	67.6	69.0	69.8	70.2	52.3	53.0	53.8	54.6	55.6	56.0	56.4
7	49.8	51.4	52.8	54.1	56.1	57.4	58.2	40.3	41.5	42.7	43.7	45.3	46.3	46.8
8	39.1	40.6	42.2	43.7	45.9	47.3	48.6	31.5	32.8	34.0	35.3	37.0	38.2	39.1
9	31.1	32.6	34.0	35.5	37.8	39.3	40.5	25.0	26.3	27.4	28.6	30.3	31.7	32.6
10	25.0	26.4	27.8	29.2	31.1	32.7	33.9	20.1	21.2	22.3	23.4	25.0	26.2	27.3
11	20.4	21.6	22.8	24.0	25.9	27.4	28.5	16.3	17.3	18.3	19.3	20.7	22.0	22.9
12	16.7	17.8	18.9	20.0	21.6	23.0	24.0	13.4	14.3	15.1	16.0	17.3	18.4	19.2
13	13.9	14.8	15.7	16.7	18.1	19.4	20.4	11.0	11.8	12.5	13.3	14.5	15.5	16.2
14	11.6	12.4	13.2	14.0	15.3	16.4	17.2	9.16	9.84	10.5	11.1	12.2	13.1	13.8
15	9.71	10.4	11.1	11.9	12.9	13.9	14.7	7.66	8.26	8.78	9.39	10.3	11.0	11.7
16	8.20	8.79	9.41	9.99	11.0	11.9	12.6	6.47	6.97	7.46	7.98	8.69	9.43	9.94
17	6.95	7.48	7.99	8.55	9.42	10.2	10.8	5.48	5.89	6.36	6.71	7.45	8.05	8.48
18	5.94	6.38	6.86	7.33	8.10	8.75	9.24	4.68	5.05	5.42	5.78	6.38	6.89	7.31
19	5.08	5.48	5.89	6.32	6.94	7.54	8.00	4.00	4.30	4.62	4.97	5.47	5.93	6.30
20	4.38	4.72	5.08	5.44	6.05	6.48	6.93	3.45	3.69	3.98	4.28	4.69	5.09	5.43
21	3.81	4.08	4.38	4.70	5.21	5.63	6.01	2.96	3.18	3.43	3.70	4.06	4.40	4.68
22	3.28	3.51	3.79	4.07	4.51	4.89	5.23	2.57	2.75	2.97	3.21	3.52	3.83	4.06
23	2.87	3.05	3.27	3.54	3.92	4.29	4.54	2.24	2.40	2.58	2.76	3.07	3.31	3.54

in the column for Homo and Hetero of Table II need to be multiplied by a factor of (85/57.6).

Some brachytherapy TPS, e.g., Plaque Simulator, based on superposition of individual seed doses, allow the user to enter distance-dependent dose correction factors to account for radiation scatter and attenuation by the gold-alloy backing and Silastic insert for a single seed. Specific recommendations for the Plaque Simulator single seed dose correction function, $T(r)$, are included in Table III, which are based on the MC results of the Hetero/Homo ratio values for a single seed (^{125}I model 6711 or ^{103}Pd model 200) at the center of a 20 mm COMS-plaque by Thomson *et al.*[59] This dose correction function accounts for scatter and attenuation by the gold-alloy backing and 1 mm path length in Silastic. Together with the ratio of the transmission factors of Silastic and water through the extra oblique path length (beyond 1 mm) in Silastic,[79] $T(r)$ is used to multiply the TG-43U1 calculated single seed dose, beginning in version 5 of PS software.

When heterogeneity-correction based TPS are used clinically,[93,96,97] careful attention must be paid to an appropriate change in prescription dose since there are no clinical results at this time demonstrating its utility. Any changes in prescription dose must evaluate the relationship between the conventional treatments with which the facility has experience and the heterogeneity-corrected dose distributions.[98] Before changing prescriptions, the clinic should gather both homogeneous and heterogeneous dosimetry for multiple patients to understand the relationship between the two dose calculation methods.

TABLE III. Values of the dose correction function $T(r)$ for a single seed in a COMS plaque at various transverse distances r from the seed center used in the Plaque Simulator calculations for ^{125}I (model 6711) and ^{103}Pd (model 200) seeds (Ref. 58).

	Dose correction function, $T(r)$	
r (mm)	^{125}I, model 6711	^{103}Pd, model 200
0	0.922	0.836
1	0.921	0.836
2	0.919	0.836
3	0.915	0.836
4	0.910	0.834
5	0.905	0.830
6	0.899	0.827
7	0.892	0.823
8	0.886	0.820
9	0.880	0.816
10	0.874	0.814
11	0.868	0.811
12	0.863	0.809
14	0.853	0.804
16	0.845	0.801
18	0.838	0.798
20	0.833	0.796
25	0.822	0.792
30	0.816	0.789
35	0.811	0.788
40	0.808	0.787

IV.C. Model specific dosimetry parameters

Appropriate repositories of dosimetry parameter data for clinical use are the published AAPM-recommended consensus data in TG-43U1 or TG-43U1S1.[27,30] An additional reference for appropriate data sources is the joint AAPM/RPC Brachytherapy Source Registry.[99] Other resources with detailed dosimetry parameter data (in excel format) are available, such as the GEC-ESTRO (Ref. 100) and the Carleton University website.[101] On the Carleton University website, Taylor and Rogers have posted MC-calculated datasets for several seed models[31,35] that include 17 $g_L(r)$ values and 5 $F(r,\theta)$ tables for $r < 10$ mm for individual seed models. The Carleton University datasets compare favorably to AAPM consensus data. Although this report focuses on ^{125}I and ^{103}Pd seeds in standard COMS-plaques, these recommendations are generalizable to all photon-emitting plaques.

As of this writing, seed models that can be made with sufficient strength for eye-plaque brachytherapy include:

- **^{125}I**: models 6711 and 9011 (Oncura, Inc., Princeton, NJ), model 2301 (Best Medical, Inc., Springfield, VA), model IAI-125A (IsoAid, LLC., Port Richey, FL), and model I25.S16 (IBt-Bebig, Berlin, Germany);
- **^{103}Pd**: model 200 (Theragenics Corporation, Buford, GA), model 2335 (Best Medical, Inc., Springfield, VA), and model IAPd-103A (IsoAid, LLC., Port Richey, FL);
- **^{131}Cs**: model CS-1 Rev2 (IsoRay Medical, Inc., Richland, WA).

The above seed models are posted on the joint AAPM-RPC Brachytherapy Source Registry, except model I25.S16 that is of the same design as model I25.S06 but with higher strength and is available in Europe.

IV.D. Image-guided brachytherapy

In support of the field of radiotherapy to implement image-guidance, the AAPM and ABS further recommend that commercial brachytherapy TPS vendors integrate tumor localization data, such as fundus photographs,[43,102–105] ultrasonographs,[106,107] and/or CT and MRI scan images[108,109] acquired before the plaque implantation. A retinal drawing should be made that includes the tumor, centered at its clock hour and anterior-posterior location as well as its basal dimensions.[105,110] In addition, the distance from the tumor edge to the central fovea and optic disc should be calculated and documented. These measurements are derived from a combination of the ophthalmic examination (slit lamp and/or ophthalmoscopy), ultrasonography (high and/or low frequency), photography, and transillumination. Each of these diagnostic/localization techniques either contributes or is critical to tumor measurement and determination of intraocular distances. Once the tumor edges and location are determined, the distances between the tumor and critical ocular structures can be calculated. These calculations may be performed with

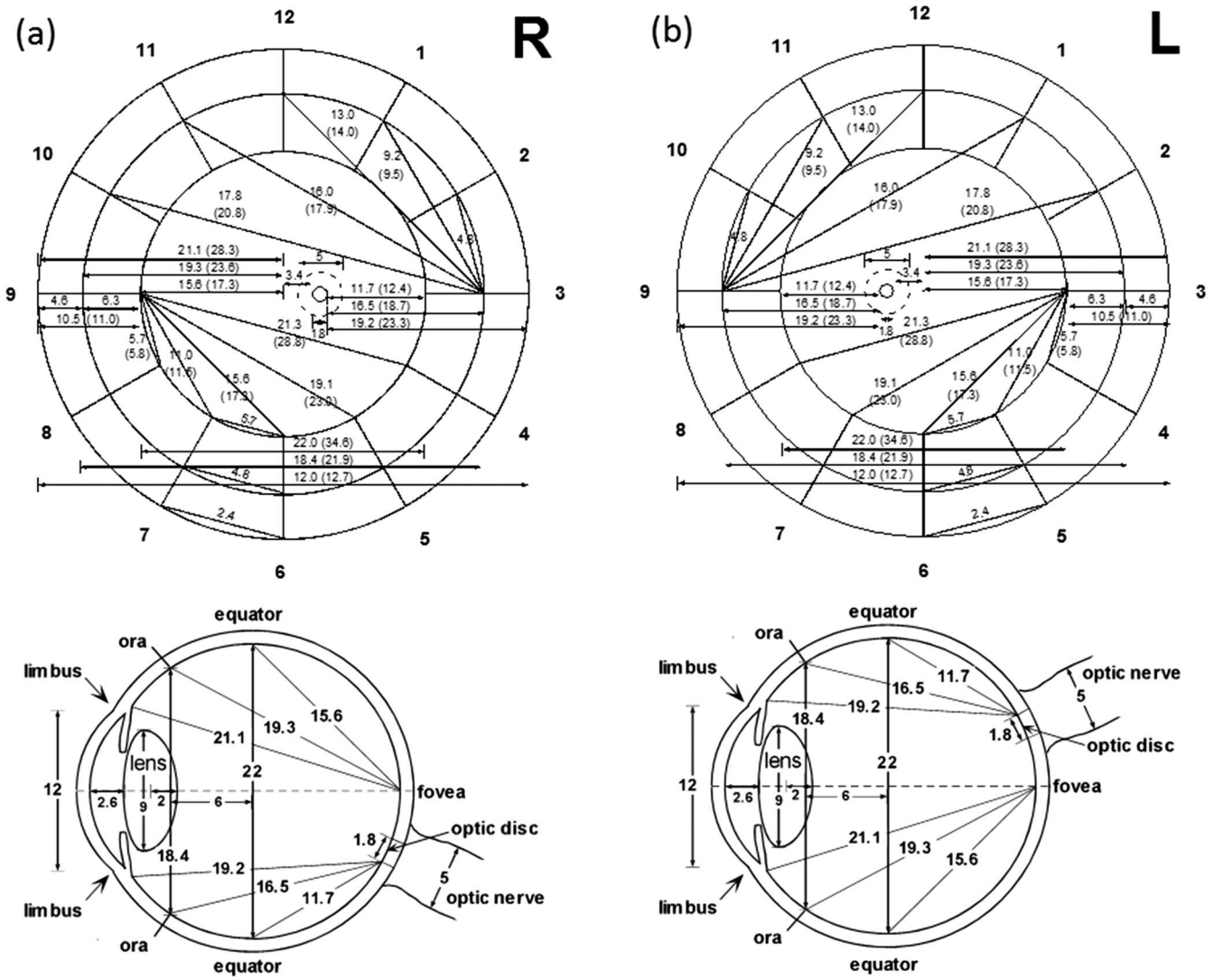

FIG. 3. Retinal/fundus diagram (upper) and transverse cross section diagram (lower) of standard eyes with 22-mm inner diameter: (a) right eye, and (b) left eye. In the fundus diagrams, the numbers indicate chord and arc lengths (in parentheses) in mm between two points in the retina. The fovea is at the center of the three concentric rings, which represent equator, ora serrata, and limbus from inside out, respectively. The small circle next to the fovea indicates the optic disc. The slightly larger dotted circle outside the optic disc indicates the projection of the outer circumference of the optic nerve sheath. The 12 clock hours indicated by numerals 1–12 (outside the outermost circle) are used to identify the locations of anatomical structures in an eye. In the cross section diagrams, only the chord lengths (in mm) are shown. Note that the actual dimensions of the eye vary and the eye is not a perfect sphere.

photographic software, ultrasound calipers, or with the retinal and cross-sectional diagrams [Figs. 3(a) and 3(b)] as used by COMS.[110,111] These diagrams were created as a guide to average normative distances from reference points within a standard eye (with a 22.0 mm inner diameter). The Radiological Physics Center (RPC) employs a method devised by Kline[112] to calculate the POI coordinates for the fovea, optic disc, and lens in the eye-plaque coordinate frame.[113]

IV.E. Quality management program

For each eye-plaque procedure, a multi-disciplinary team consisting of at least one ophthalmologist, one radiation oncologist, and one clinical medical physicist or designate (such as a medical dosimetrist) should work closely together to assure safe, accurate, and effective brachytherapy. General quality checks and QA for individual patient cases are necessary at different stages of the treatment process as outlined below.

IV.E.1. Commissioning

The ultrasound device used for determining tumor size and extent should be tested using the procedures recommended by AAPM Ultrasound TG-1.[114] An institution must have a well-type ion chamber with a traceable calibration to a national metrology institute (e.g., NIST, NPL, PTB, etc.)[115] to determine brachytherapy source strengths (in terms of air kerma strength, not apparent activity)[116] prior to plaque assembly and application. The well chamber should be recalibrated by an accredited dosimetry calibration laboratory (ADCL) or a national metrology institute (e.g., NIST) at 2-year intervals.[117]

Upon receipt of the gold-alloy backing and Silastic inserts, the location of the grooves on the Silastic insert should be verified against the diagram in Fig. 1. As a first step preparing to commission the eye-plaque TPS, the values of seed coordinates (Table I) entered in the TPS should be verified for accuracy for all available plaques in the clinic. Second, the clinical medical physicist should validate the single source dosimetry data (Sec. IV.C) in the TPS. Preceding clinical use, the eye-plaque brachytherapy TPS should be commissioned according to TG-53.[118] There are notable differences amongst brachytherapy TPS in the amount and format of dosimetry parameter data that can be entered. For eye-plaque dosimetry, $g_L(r)$ should be specified with r resolution of 1 mm or finer for 1 mm $\leq r \leq$ 30 mm to ensure accurate dose-rate determination at clinically relevant distances. Similarly, $F(r, \theta)$ should be defined at 10° or smaller increments of polar angle, and include data for at least two radial distances of $r < 10$ mm. While brachytherapy TPS vendors improve dose calculation capabilities, the AAPM and ABS recommend that clinical medical physicists calculate central-axis homogeneous dose distributions for either the ^{125}I model 6711 or ^{103}Pd model 200 sources in a 16 mm COMS plaque to compare with published dose distributions.[90] The clinical medical physicist should also estimate central-axis inhomogeneous dose distributions for these same sources for comparison if the brachytherapy TPS in that institution allows such calculations.[90]

IV.E.2. Preoperative planning

Upon the decision to treat a specific patient, agreement as to which radionuclide and source model to use should be reached among the radiation oncologist, ophthalmic oncologist, and the clinical medical physicist. This decision may be based on preoperative comparative treatment planning to determine doses to the tumor and to normal ocular structures (e.g., fovea, optic disc, lens, opposite eye wall). Each radiotherapy patient record should include a retinal diagram that indicates the affected eye, tumor location, tumor dimensions, and proximity to critical normal ocular structures.[105] A prescription should be used to initiate the treatment planning process. It should indicate the affected eye (left or right), prescription dose, prescription point, initial dose rate at the prescription point in Gy/h, radionuclide, half-life, seed model, number of seeds, seed strength, plaque type and size, GTV-to-PTV margin (e.g., 2 mm), implant and explant dates, and treatment duration. The magnitude of the heterogeneity correction on the central axis can be calculated using data in Table II. In addition to the prescription point on the central axis, dose to the fovea, optic nerve, lens, and opposite eye wall as well as the outer and inner sclera along the plaque central axis should be determined as accurately as possible given the available resources in the clinic. If a heterogeneity correction model is available, then heterogeneity corrected doses should be documented as calculated. At a minimum, doses to points (fovea, optic disc, lens, opposite eye wall and sclera) should be calculated using the homogeneous models and an estimate of the heterogeneity correction noted using the dosimetry data presented in this report as a guideline.

The brachytherapy plan should be checked by another qualified physicist or dosimetrist and the TG-43 based dose distribution should be verified by an independent dose calculation method such as a spreadsheet calculation or using third-party commercial software. Tolerances of ±2% on the plaque central axis may be considered acceptable.

IV.E.3. Preoperative quality assurance

An in-house clinical medical physicist or his/her assigned designate (such as a medical dosimetrist) should verify the seed strengths prior to plaque assembly using a well chamber with a traceable calibration to a national standard established by a national metrology institute (e.g., NIST) following recommendations by the AAPM Low Energy Brachytherapy Source Calibration Working Group.[115] Guidance on the actions to be taken based on the percentage difference found between the manufacturer's source-strength certificate and the in-house assay is provided by Butler *et al*. Ten randomly selected seeds from each source-strength grouping should be measured; all seeds should be measured for seed batches <10. A tolerance of 6% should be used as given in the top-third of Table II of Butler *et al.* for calibration agreement with the manufacturer's certificate. This Task Group is also in agreement with Sec. II.B of Butler *et al.* that a tolerance of 3% for the batch mean should be used.

The seed loading pattern in the Silastic insert for the individual patient case should be confirmed using autoradiography,[119] photography, or visually inspected (and documented) by a person different than who loaded the plaque. To minimize personnel radiation exposure, established time/distance/shielding practice should be followed. Due to the low-energy photons associated with sources used for eye plaque brachytherapy, use of a high-Z transparent shield can permit handling of the plaque and sources while minimizing whole-body exposure. Radiation survey instruments should be calibrated for the appropriate energy since response to ^{137}Cs may be a factor of 2 lower than for low-energy sources.

While the seeds need not be sterilized before plaque assembly, the plaque must be sterilized after its assembly prior to implantation. Methods of plaque sterilization are determined according to hospital-approved procedures and include steam, gas, and chemical techniques.[38] Radioactive plaques must be transported within a shielded container marked with radiation safety labels, the radionuclide, and the patient's name. Pertinent laws and hospital radiation safety requirements should be reviewed in advance with the patient and his/her family.

A recent development has been the availability of prepared plaques for rent from source manufacturers. These plaques come sterilized with no opportunity for direct measurement of source strength or loading confirmation. A minimum of one nonsterile loose seed should be ordered and assayed by the in-house physicist, given that the number of seeds ranges from 5 to 24 in fully loaded 10 mm–22 mm COMS plaques. The assay tolerance for the air kerma strength of the loose seed(s) is 6% individually and 3% for any single batch. The recom-

mended number of seeds and tolerance matches that described in the Butler *et al.*[115]

IV.E.4. Operative environment

Before or at the time of anesthesia and the brachytherapy implant, the patient should be provided an identity wristband including the patient name, medical record number, and the attending physician's name. The patient's records should be available and reviewed prior to implantation. The correct eye and tumor location within the eye should be confirmed by clinical examination, e.g., indirect ophthalmoscopy. Familiarity with the ophthalmology terms oculus dexter (OD) and oculus sinister (OS) for right and left eye, respectively, may assist with correct eye identification. A timeout procedure should be performed before starting the implantation operation to verify the aforementioned information. To provide radioactivity accountability, staff exiting the operating room after the procedure has started should be inspected with a radiation survey meter to prevent migration of radioactive seeds that may have been accidentally removed from the plaque.

The largest uncertainty in the source location relative to patient anatomy involves the plaque placement by the surgeon. Intra-operative ultrasonographic imaging, scleral depression, and/or transillumination techniques are common and widely used to verify the accuracy of plaque placement for posterior ocular tumors.[120,121] If used, ultrasound imaging should be performed along both the longitudinal and transverse meridians in 2D or 3D.[122] Printout of a polar map of the retinal diagram from Plaque Simulator showing the locations of the suture holes relative to ocular landmarks can aid the suturing and plaque-placement verification processes. A copy of these images and the operative report should be placed in the patient record.

The prescription should indicate the circumstances of plaque application, with any differences from the intended plan noted. A suitable radiation survey meter should be used to evaluate the operating room before and after the procedure. This meter should be calibrated for the radionuclide used or an appropriate correction factor should be established, and the formalism of NUREG-1556 or an equivalent formalism should be followed.[123] The room and all staff should be surveyed following completion of plaque placement. The exposure rate at 1 m from the patient/implant should be assessed and documented according to NRC or agreement state regulatory requirements. While unlikely, seeds may separate from the plaque prior to, during, or after surgery. Thus, all radioactive sources should be accounted for (either implanted or placed in a shielded container) at the conclusion of surgery. Radiation survey in the operating room should also be performed after the patient leaves the room to ensure no radioactive sources are left behind.

IV.E.5. Postoperative

Should the patient be discharged after plaque placement, the patient should be given wound care instructions, emergency contact information, and information on the radionuclide and source strength implanted. This is done (in part) for other medical professionals who may see the patient in an emergency room or at other medical offices. This information should also include acceptable distances and times for proximity to other people, especially children.[124] The patient should be provided with a lead patch for protecting the public from radiation exposure. The patient should be reminded to return on a specific date for plaque removal surgery. There should be an action plan developed to return the patient for plaque removal in the case of severe weather, national or local emergency, or patient noncompliance, and for plaque retrieval should the patient unexpectedly expire or if a seed unexpectedly comes loose following plaque placement.

V. DISCUSSION

Accuracy of dose calculations is necessary because radiation response is highly dependent on dose, and the dose response can have a steep gradient especially in the therapeutic range. Accurate dose calculations are the foundation upon which meaningful intercomparisons can be performed amongst different radiation modalities and for perturbations related to treatment variables such as the use or nonuse of Silastic inserts, gold "seed-guides," seed slots, notches, plaque-slots, and custom plaque designs. Thus, as more accurate methods for dose calculation become available, these methods should be adopted clinically even though the changes may temporarily unsettle the clinical practice. This report addresses the issues that arise when a new dose calculation method is adopted in a well-established clinical application.

A prescription dose of 85 Gy at 5 mm depth was used in Table II of this report as a reference dose value for the homogeneous water assumption. When the prescription point is the tumor apex at a depth different from 5 mm, the tabulated dose values should be renormalized to the requested prescription dose at the requested prescription depth with the homogeneous water assumption and all other dose values rescaled accordingly. Note that the ABS recommendation[38] of the prescription depth is at the tumor apex, including the tumors with apex height less than 5 mm. This is different from the original recommendation of minimum 85 Gy to 5 mm prescription dose required by the COMS group.[20,21,24] Some centers have reported even lower apical tumor prescription doses for choroidal melanoma, retinoblastoma, and select choroidal hemangiomas.[14,125–127]

The AAPM and ABS recognize that advances in ophthalmology and radiation oncology have improved tumor control and eye retention, and also strive for vision preservation.[3,12,13,19] With these endpoints and goals, other plaque designs and alternative radiation modalities are being evaluated. For example, when treating tumors close to or surrounding the optic nerve, a notch or slot can be cut from standard gold COMS-plaques.[24,51] Similarly, COMS plaques have been modified to decrease dose to critical structures such as the cornea, iris, and lens.[43,53] Other design variations include ROPES, USC, IBt/Bebig (beta-emitters), Nag, other custom made plaques, and a "seed-guide insert" that can be used to locate brachytherapy sources in the COMS

gold-alloy backing without Silastic insert.[50] Further, the AAPM and ABS recognize that standardized methods of dose calculation will facilitate multi-institutional analysis of treatment efficacy and side effects. Thus, it is important to use identical nomenclature, tumor-staging and most importantly, standardized dosimetry practices.[128]

While the Appendix reviews clinical aspects of eye-plaque brachytherapy, it does not address the influence of dose rate and dose-gradient or low-energy photon relative biological effectiveness (RBE), effects that should be considered when varying implant duration or comparing eye plaque brachytherapy to other radiotherapy modalities. The above-mentioned effects are under investigation.[129,130] Further, the dosimetric analysis performed for the current report does not consider the tissue-heterogeneity of the structures in and around the eye; further analysis is needed to evaluate these factors.[59]

Image guidance for eye-plaque brachytherapy based on fundus photography/ophthalmoscopy and ultrasonography has been developed and used in the COMS study in the localization and delineation of eye tumors. It should be noted that the optics and images are affected by eye size, tumor specific characteristics, and pigmentation. For example, the edges of some choroidal melanomas dive deep to the choroid and (by ophthalmoscopy) appear only as a mild normally pigmented elevation of the retina. In these cases, ophthalmoscopy may reveal normal yet elevated retina; while ultrasonographic measurement better confirms the actual basal tumor dimensions. Similarly, photographically based fluorescein or indocyanine green angiography will occasionally reveal a larger than expected tumor basal dimension.[131,132] Current CT and MRI images are limited in spatial resolution and accuracy for ocular tumor delineation. With the future developments of high-resolution (sub-millimeter) imaging and integration of multiple image datasets, it will be possible to accurately outline the tumor and the normal structures in 3D. At that time, consideration should be given to 3D image-based treatment planning, DVHs, and other modern treatment planning tools as commonly used for external beam radiation therapy.

ACKNOWLEDGMENTS

The authors thank Dr. Charles Coffey, Dr. Heath Odau, and the reviewers throughout the AAPM, ABS, and *Medical Physics* review process for their constructive comments and timely feedback for improving this report.

APPENDIX: CLINICAL ASPECTS

In this appendix, the historical evolution of eye-plaque brachytherapy as well as the most recent ABS recommendations for treatment of choroidal melanoma are presented. Further, the concepts of relative intraocular dose-gradients, the optic nerve as an obstruction to plaque placement, and innovative plaque designs (for iris and peripapillary tumors) are described. Lastly, a brief review of the clinical outcomes derived from widely used ^{125}I, ^{103}Pd, ^{106}Ru/^{106}Rh plaque and charged particle therapies as well as less commonly employed sources are presented.

1. Local control and radiation side effects

Five-year local control rates for eye-plaque therapy or external beam therapy using protons are excellent, with a range of 81%–97% in Table 4 of Finger *et al.*[125] Thus, current ocular melanoma research efforts aim to reduce side-effects to normal tissues, such as eye lash loss, dry eye, corneal damage, radiation retinopathy, radiation optic neuropathy, vitreous hemorrhage, cataract, and neovascular glaucoma.[3]

Radiation-related vision loss is typically due to cataract, radiation maculopathy, optic neuropathy, exudative retinal detachments, or neovascular glaucoma.[3] In the treatment of juxtafoveal and subfoveal tumors, foveal chorioretinal atrophy can also lead to severe irreversible loss of vision. In general, the higher the radiation dose to the fovea, the faster the onset of chorioretinal atrophy and loss of central vision.[12,133,134] In addition, high-radiation doses to the sclera, choroid, and retina are more likely to cause secondary retinal detachments with associated vision loss.[135] Finger noted that plaque location is related to the incidence of cataract and retinopathy after brachytherapy.[12,13] However, in multivariate analysis it appears that doses to fovea and lens are the most significant factors.[12,133,134] Note that the doses quoted in the studies mentioned in this appendix are pre-TG-129 values.

Radiation retinopathy and optic neuropathy are progressive vascular diseases characterized by micro-aneurysm formation, neovascularization, and large and small vessel leakage. Clinical findings include small infarcts called "cotton-wool spots" for their appearance, hemorrhages, and deposits of exudates, e.g., fat. Serum leaking from normal and neovascular blood vessels causes retinal or optic nerve edema, vision loss, and ischemia. Over time, small and large blood vessels close, which leads to progressive ischemia. Current research suggests that vascular endothelial growth factor (VEGF) increases retinal vascular permeability and contributes to radiation retinopathy and optic neuropathy.[136–139]

The optic nerve is particularly vulnerable to radiation morbidity. It travels from the eye through a fixed scleral opening into the orbit. As radiation damage makes the intraneural blood vessels progressively incompetent, components extravasate into the optic nerve, expanding in volume within a confined scleral space. Clinically viewed as papilledema within the eye, optic nerve incarceration leads to further ischemia and eventual atrophy. This process also appears to be partially mediated by VEGF. Finger and co-workers performed the first pilot studies examining the effects of anti-VEGF medications for radiation maculopathy and optic neuropathy.[137,138,140] Since anti-VEGF medications have been shown to suppress neovascularization and decrease leakage from both normal and abnormal vessels, intraocular (intravitreal) injections of bevacizumab (Avastin) or ranibizumab (Lucentis) by Roche-Genentech, Inc., (South San Francisco, California) have been used to ameliorate radiation-associated optic nerve and macular edema as well as hemorrhage after ^{125}I and ^{103}Pd plaque brachytherapy.[137,139,141]

2. 2003 ABS guidance

The ABS made recommendations for patient selection, treatment techniques, prescription dose, and dose rates for eye-plaque therapy of uveal melanoma.[38] They recommended that most patients with COMS small-sized uveal melanomas (<2.5 mm height and <10 mm in largest basal dimension) be candidates for plaque brachytherapy if evidence of growth was observed. Patients clinically diagnosed with COMS medium-sized uveal melanomas (2.5 mm–10 mm in height and ≤16 mm basal diameter) were candidates for plaque brachytherapy, while some patients with COMS large-sized melanomas (>10 mm height or >16 mm basal diameter) could also be treated with plaque brachytherapy. In general, plaque brachytherapy was an option for all patients free of metastatic disease and able to tolerate surgery. Histopathologic verification of the primary tumor diagnosis was not required. According to the ABS, patients with gross-extrascleral extension, ring melanoma, and tumor involvement of more than half of the ciliary body were not suitable for plaque therapy. While recommendations pertained to ^{125}I sources, other radionuclides were reviewed in the report. The ABS recommended a minimum dose of 85 Gy to the tumor apex using the AAPM TG-43 formalism for dose calculations assuming an unbounded homogeneous water medium (including the NIST99 calibration standard). ABS recommended a dose rate of 0.60 Gy/h–1.05 Gy/h which would deliver the total dose in 3–7 consecutive days.[38] The 2003 ABS recommendation eliminated the minimum 5 mm depth for the prescription point that was mandated within the COMS.

3. Dose gradient

The ABS recommended that the tumor apex be targeted to receive 85 Gy.[38] The apex is defined as the farthest intraocular extent of the tumor, so tissue proximal to that point will receive progressively more than 85 Gy. The tumor base typically receives the maximum dose due to source proximity. As Finger pointed out in 1997, during plaque radiation therapy a steep dose gradient exists within the tumor.[3]

Since a dose gradient exists, plaque brachytherapy of two unequally sized ocular tumors would result in strikingly different values for the dose maxima in the tumor volume. For example, a dose of 85 Gy to the apex using an ^{125}I plaque brachytherapy for a 10 mm thick tumor may result in a central-axis inner-scleral dose of 644 Gy (a base-to-apex ratio of 8 to 1); this inner-scleral dose will reduce to 166 Gy for a 3 mm thick tumor (a base-to-apex ratio of 2 to 1).[90] While the mean tumor dose for the former is much higher than that of the latter, these two treatments are currently considered equivalent. This phenomenon is particularly important in treatment of tumors close to the fovea and/or optic nerve where higher doses to regions of concern correlate with a higher incidence of radiation maculopathy and optic neuropathy.[51,57,133,134,141,142]

The dose gradient is also affected by radionuclide selection, source design, and plaque component construction. For example, treatment of a 5-mm thick tumor using beta-emitting ^{106}Ru/^{106}Rh plaques delivers a base-to-apex dose ratio of approximately 9 to 1 compared with 3 to 1 for ^{125}I.[3] For an apex dose of 85 Gy, with ^{106}Ru/^{106}Rh the base can receive almost 800 Gy as opposed to 260 Gy for ^{125}I. This high base-to-apex dose ratio may explain why patients treated with ^{106}Ru/^{106}Rh plaques are more likely to develop chorioretinal atrophy around the tumor, less commonly seen after ^{125}I or ^{103}Pd plaque therapy.[143]

For treatment of equivalent-sized tumors, lower energy ^{103}Pd (21 keV) versus ^{125}I (28 keV) or ^{131}Cs (30 keV) will progressively increase the dose gradient, but not as much as the beta-emitting ^{106}Ru/^{106}Rh. In general, ^{103}Pd will increase the dose within the target volume and decrease dose to most normal ocular structures outside the tumor volume except the sclera. Preoperative comparative dosimetry studies indicate that treatment with different radionuclides results in differing scleral, choroidal, and retinal doses.

It is important to consider dose to normal ocular structures, because side effects may be predicted based on these measurements.[12,13,134] However, there exist no current recommendations for maximum doses to the lens, macula, optic nerve, or sclera. Similarly, there exists no dose escalation study to determine the required base or apex dose for any intraocular tumor.[144] These facts underscore the need for improved dosimetry methods to allow more accurate research on the radiation tolerance of normal ocular structures and the minimum required dose for tumor control. Research is needed to decrease irradiation of normal ocular structures, to reduce the apex dose, to increase the dose gradient outside the tumor, and to reduce the target volume.

As discussed above, dose distributions vary amongst low-energy photon-emitters for the same tumor, but there is limited clinical data comparing the efficacy of ^{125}I versus ^{103}Pd eye plaques.[145] In 1991, Finger *et al.* compared the radiation distribution of ^{103}Pd versus ^{125}I brachytherapy plaques sewn to 12 human donor eyes.[146] This experiment involved placing equivalent arrays of ^{103}Pd or ^{125}I seeds into standard 14 mm COMS-plaques. The plaques were placed to approximate nasal and temporal equator placement. Three sets of two TLDs were used to quantify radiation delivered by the brachytherapy plaques. Dosimeters were sewn to the eye in three target locations: on the center of the cornea, on the sclera beneath the macula, and at the equator in a position opposite the plaque. After adjusting ^{103}Pd source strengths for the same ^{125}I prescription dose, ^{103}Pd plaques were found to deliver less radiation to all three target locations.[146] Subsequent comparative clinical dosimetry also reflected this difference.[145] In these cases, preoperative simulations comparing equal apex tumor doses revealed that ^{103}Pd brachytherapy plaques delivered more dose to the tumor and less dose to most normal ocular structures in comparison to ^{125}I eye plaques. These findings are consistent with the MC simulations as mentioned in Secs. I–IV.[90]

4. ^{125}I and ^{103}Pd plaque outcome studies

Introduced by Rotman, Packer, and Sealy in the 1970s, clinical experience with ^{125}I eye plaques has

been described by many investigators, most notably by COMS.[15,19,39,40,42,54,79,147–150] The most recent COMS publications of randomized multicenter clinical trials using ^{125}I brachytherapy versus enucleation for COMS-medium sized choroidal melanoma reports 12-year mortality rates and prognostic factors.[19] All patients were followed for 5–15 years at scheduled examinations for metastasis or another cancer until death. Out of the 1317 enrolled patients, 515 patients were eligible for 12 years of follow-up, with 231 patients (45%) still alive and clinically cancer-free. For patients in both treatment arms, 5- and 10-year all-cause mortality rates were 19% and 35%, respectively; by 12 years, the cumulative all-cause mortality rate was 43% among patients in the ^{125}I brachytherapy arm and 41% among those in the enucleation arm. The 12-year death rate with histopathologically confirmed melanoma metastasis was 21% in the ^{125}I brachytherapy arm and 17% in the enucleation arm. In multivariate analysis, the most significant predictors of time to death from all causes and death with melanoma metastasis were increased patient age and larger basal tumor diameter. This 12-year follow-up data confirmed earlier COMS reports. It was the conclusion of the COMS Study Group that there was no significant difference in survival for patients treated by ^{125}I brachytherapy or enucleation.[19,151]

For ^{103}Pd, the most extensive outcome studies have been described by Finger, Chin, and Duvall in the Palladium-103 for Choroidal Melanoma Study Group.[125] They reported 18-year experience with ^{103}Pd in a retrospective series from 1990 to 2007 with four hundred patients diagnosed with uveal melanoma and negative for metastatic disease. ^{103}Pd plaque brachytherapy was delivered to a mean apex radiation dose of 73.3 Gy over 5–7 continuous days. Patients were evaluated for local tumor control, visual acuity, radiation damage (retinopathy, optic neuropathy, cataract), and metastatic disease. A total of 272 tumors (68%) were located at or posterior to the equator. According to the 7th edition AJCC classification for uveal melanoma, there were 186 (46.5%) T1 tumors, 156 (39%) T2 tumors, 50 (12.5%) T3 tumors, and 8 (2%) T4 tumors. Alternatively these tumors could be classified as COMS-small (3%), COMS-medium (92%) and COMS-large (5%).[125,128] Patients were followed for a maximum of 205 months with a mean follow-up of 51 months. Fourteen patients required salvage enucleation, including five for tumor growth and nine for glaucoma pain control. The local control rate was 97%. Life-table analysis of patients with 20/200 or better vision before treatment ($n = 357$) suggests that 79% and 69% are expected to retain that acuity for 5 and 10 years, respectively. These data stand in contrast to other reported series.[3,4,18,19,42,47,143,150,152–158] Life-table analyses demonstrate a probability that 92.7% and 86.6% of patients will be free of metastatic disease at 5 and 10 years, respectively. Finger *et al.* concluded that ^{103}Pd plaque brachytherapy used to treat 400 patients with uveal melanoma in this series provided clinical results superior to those reported for alternative forms of radiation.[125] However, determination of statistically significant differences between the use of ^{103}Pd and ^{125}I would require a case-matched or prospective randomized multi-institutional clinical trial.

5. Iris and iridociliary melanomas

Previously treated by surgical removal, i.e., iridectomy or iridocyclectomy, there has been a trend away from intraocular surgery of anterior uveal melanomas toward the relatively safe extraocular application of brachytherapy plaques. Plaque therapy avoids the risks of intraocular surgery, including infection, hemorrhage, acute cataract, and retinal detachment. In contrast to surgical removal, anterior plaque brachytherapy offers iris retention, retained iris function, decreased glare, and larger treatment margins.[159]

Iris and iridociliary melanomas can be measured accurately using high-frequency ultrasound also called "ultrasound biomicroscopy."[160–163] Introduced in 1991, ultrasound frequencies of 35 MHz–50 MHz permitted high-resolution imaging of tumors in the posterior iris and ciliary body. High-frequency ultrasound measurements of iridociliary tumor size and apex height allowed for improved plaque-size selection, treatment planning, and tumor follow-up.[155,159,164]

With 10-year follow-up, epi-corneal plaque brachytherapy was associated with excellent local control, high-risk of radiation cataract formation, and low-risk for radiation retinopathy or optic neuropathy, although, it was an uncomfortable treatment modality for the patient. More recently, 0.1-mm thick donor amniotic membrane grafts have become commercially available (Biotissue, Inc., Miami, FL).[165] During insertion, the membrane can be placed between the plaque and cornea as a buffer to reduce discomfort.[166]

6. Peri-, juxta-, and circumpapillary melanomas

The optic nerve presents a significant obstruction to plaque placement and effective tumor control for tumors near the optic nerve. The optic nerve, as the disc observed within the eye, has a mean diameter of 1.75 mm. However, immediately posterior to the eye where it is surrounded by the optic nerve sheath, it expands to a mean diameter of 5 mm.[167] Therefore, it is physically impossible even with "perfect" plaque placement to cover the posterior margin of a choroidal melanoma that extends within 1.5 mm of the intraocular portion of the nerve (the optic disc) with standard or notched COMS-plaques. In the past, plaque brachytherapy for juxtapapillary melanomas relied on side-scatter and plaque-tilt to treat posterior margins.[3,18,120,121] Efforts to address this problem have included plaque-notching, removal of the plaque posterior lip, and adjuvant transpupillary thermotherapy (TTT) laser to the untreated peripapillary tumor.[57,168] Despite customized-notched plaques and adjuvant laser, patients with peripapillary, juxtapapillary, and circumpapillary melanomas have been reported to exhibit relatively poor local tumor control.[18,142,143]

In 2005, an approach was developed to measure the retrobulbar optic nerve sheath diameter (ONSD) with 3D ultrasound to permit plaque irradiation of tumors near or surrounding the optic disc.[51] Given the ONSD was typically 5 mm–6 mm, conventional plaques with gold-alloy backing were altered to accommodate the nerve within the plaque. Eight millimeters wide, variable-depth slots with parallel sides were cut

into standard COMS-plaques. Unlike pie-shaped notches that merely move the plaque slightly closer to the posterior edge of the tumor, slotted plaques accommodate the retrobulbar optic nerve into the slot and enable the targeted zone to include the entire tumor and 2 mm–3 mm free margin (as is used for more anterior choroidal melanomas).[51] The 5-year follow-up results of these slotted plaques were recently published.[57]

However, slotted plaque dosimetry presents additional challenges. Brachytherapy seeds cannot be placed within the slot and are instead affixed in nonstandard patterns around the slot. Dose distributions from the seeds are expected to fill in the gap created by the slot to encompass the juxtapapillary and posterior tumor margins with radiation dose. Careful, preoperative dosimetry is required to ensure that the targeted zone (tumor and free-margin) within the slot receive an adequate dose.[57]

Slotted plaques can enhance plaque placement. Although the most posterior portion of the eye can be a challenging location for plaque localization, the optic nerve also serves as a fixed reference within the plaque that can aid proper plaque placement.[57] Confirmatory, intraoperative ultrasound imaging was suggested by the investigators.[121,122] In this study, radiation optic neuropathy and maculopathy were found treatable with intravitreal anti-VEGF therapy.[139–141]

Slotted plaques and future customized eye-plaque innovations may improve local control, diminish irradiation of normal tissues, and retain eyes.[57] However, these deviations from standard plaque construction and dosimetry warrant further investigation by clinical medical physicists.

7. Large and extra-large uveal melanomas

Since 2003, when the ABS suggested that COMS large tumors, i.e., tumors $>$ 16 mm in basal diameter and or $>$ 10 mm in height, are typically treated by eye removal (enucleation), there has been a trend toward offering brachytherapy as an enucleation alternative for eye and vision sparing.[38] Many of these tumors would be graded as T2, T3, or T4 by the 7th edition AJCC staging manual.[128] In these cases, standardized COMS 22 mm and custom-made 22 mm and 24 mm gold-alloy plaques have been employed. As might be expected, vision retention has been complicated by a greater incidence of synchronous retinal detachments, hemorrhages, intraocular inflammation, and glaucoma commonly associated with tumors of this size.[169] However, studies have found acceptable eye and vision retention rates, and most patients would prefer to retain their eye—even with partial or complete vision loss.[47,48,170,171]

8. Alternative radiation modalities

Though several publications on clinical outcomes have been published, there are no prospective, randomized clinical trials comparing the clinical outcomes among plaque and external beam radiotherapy modalities for choroidal melanoma. Alternative radiation modalities include external-beam therapy with protons or helium ions from high energy cyclotrons, megavoltage energy photons from linear accelerators or Gamma Knife® (^{60}Co), and beta-emtting ^{106}Ru/^{106}Rh plaques.

a. Protons and other heavy charged particles

Ocular melanoma proton therapy was pioneered at the Harvard Cyclotron Laboratory, Massachusetts Eye and Ear Infirmary, and Massachusetts General Hospital.[5–7] Currently at least 13 institutions around the world are using protons to treat ocular tumors.[172] Recently, treatments have been given over 4 consecutive days and four treatment fractions to a prescription dose of 60 Gy or less using a proton RBE of 1.1 in comparison to ^{60}Co. Proton therapy is effective for local tumor control with several groups reporting rates of 89%–98%.[8,10,173,174] Five-year survival rates of 80% with preservation of the globe and functional vision have been published.[172,173] Unlike low-energy plaque therapy, proton therapy typically requires an anterior entrance dose with more commonly reported anterior segment complications, including lash loss, dry eye, neovascular glaucoma, and cataract.[3] Also unlike plaques, treatment can be confounded by eye movement leading to a mobile target volume and potential for geographic miss. It is difficult to equate high dose-rate therapies, such as proton irradiation to low dose-rate brachytherapy. Only two comparative studies have been performed: Hungerford and Wilson compared protons to ^{125}I and ^{106}Ru/^{106}Rh,[8,9] and Char *et al.* examined helium-ions versus ^{125}I.[10] While both studies reported good local tumor control and reasonable vision retention in comparison to ^{125}I, secondary enucleation rates for proton and helium ion therapy were higher than for radionuclide-based therapy.

b. Linear accelerators

External beam photons have been used for over 30 years for the treatment of choroidal melanoma with mixed results.[175,176] Treatments over 5–7 days with five treatment fractions delivering 50 Gy–70 Gy with 6 MV arcs are most commonly employed. Outcomes have included favorable local control rates, yet with high rates of enucleation and vision degradation, attributed mainly to the larger mean lesions sizes, than those treated with beta-emitting or low-energy photon-emitting radionuclides. With the radiation source positioned approximately 1000 times further from the eye than for plaque brachytherapy, patient immobilization and treatment delivery are challenging aspects of this treatment modality.[177,178]

c. Gamma Knife

Photons from ^{60}Co have been used in Gamma Knife® (Elekta, Stockholm, Sweden) to control the growth of choroidal melanoma using a single dose of 20 Gy–25 Gy to the 50% isodose line. Relatively few patients have been irradiated using the Gamma Knife, mostly for juxtapapillary tumors.[179–184] Similar to charged particle therapy, Gamma Knife treatment can be complicated by eye movement and

high dose-rate effects. Techniques such as surgical fixation of the ocular muscles or ocular suction stabilization devices have been used to limit eye movement.

d. ^{106}Ru/^{106}Rh eye plaques

Mostly in Europe, ^{106}Ru/^{106}Rh plaques are the most cost-effective treatment modality. The beta-emitting ^{106}Ru/^{106}Rh eye plaques were pioneered by Lommatzsch in Germany.[142] Twenty-year follow-up for posterior tumors was reported in 2000.[143] In 1999, Wilson and Hungerford reported on a retrospective, nonrandomized chart review for choroidal melanoma patients treated with ^{125}I, ^{106}Ru/^{106}Rh, and protons, concluding that local control rates are better for ^{125}I and protons (95%) than ^{106}Ru/^{106}Rh (89%). However, ^{106}Ru/^{106}Rh had fewer ocular side effects.[9]

^{106}Ru/^{106}Rh has a long half-life of 371.6 days and high-energy beta particles (3.54 MeV maximum energy, 1.42 MeV mean energy). The percent depth dose in tissue is approximately 5%–10% at 7 mm depth, depending on plaque size and shape. The radioactive material ^{106}Ru/^{106}Rh is encapsulated in a curved silver plaque in various shapes and dimensions available from IBt-Bebig. The ^{106}Ru/^{106}Rh is electrodeposited on a 0.2 mm thick Ag substrate mounted on to a 0.7-mm Ag backing and covered with a 0.1-mm thick Ag window. The dosimetry studies for such plaque design have been reported in the literature.[44,45,72,77,78,80,85,185–188] Due to the limited penetration of beta particles, many centers limit treatment to tumors less than 5 mm in apex height due to the limited range of ^{106}Ru/^{106}Rh electrons. Compared to ^{125}I or ^{103}Pd, ^{106}Ru/^{106}Rh plaque therapy is associated with a much higher inner scleral dose, often inducing peri-tumoral chorioretinal atrophy and more rapid vision loss after treatment of perifoveal tumors. In addition, ^{106}Ru/^{106}Rh plaques have a very sharp penumbra that is likely responsible for reported failures of local control in treatment of juxtapapillary tumors that have required side scatter for local control.[142,153,156] However, there are likely to be fewer significant side-effects and excellent vision-sparing with using ^{106}Ru/^{106}Rh in treatment of small-height tumors away from the optic nerve and macula because of this sharp penumbra. The sharp penumbral demarcation at the edge of a ^{106}Ru/^{106}Rh plaque therapy targeted zone also requires more surgical skill. ^{125}I or ^{103}Pd plaques offer more lateral radiation scatter toward limiting the risk of geographic miss. These differences are typically addressed by using relatively larger ^{106}Ru/^{106}Rh plaques so as to increase the size of the tumor-free margins. Due to the risks of misapplication, ^{106}Ru/^{106}Rh plaques should be placed by experienced plaque surgeons.

[a]Electronic mail: soutung@gmail.com

[1]R. Moore, "Choroidal sarcoma treated by the intraocular insertion of radon seeds," Br. J. Ophthalmol. **14**, 145–156 (1930).
[2]H. B. Stallard, "Radiotherapy for malignant melanoma of the choroid," Br. J. Ophthalmol. **50**, 147–155 (1966).
[3]P. T. Finger, "Radiation therapy for choroidal melanoma," Surv. Ophthalmol. **42**, 215–232 (1997).
[4]K. Leonard, E. Bannon, J. Mignano, J. Duker, N. Gagne, and M. Rivard, "Eye plaque brachytherapy for the treatment of uveal melanoma: The 2010 Tufts Medical Center experience," Int. J. Radiat. Oncol., Biol. Phys. **78S**, S268 (2010).
[5]E. S. Gragoudas, M. Goitein, A. M. Koehler, L. Verhey, J. Tepper, H. D. Suit, R. Brockhurst, and I. J. Constable, "Proton irradiation of small choroidal malignant melanomas," Am. J. Ophthalmol. **83**, 665–673 (1977).
[6]E. S. Gragoudas, M. Goitein, L. Verhey, J. Munzenreider, M. Urie, H. Suit, and A. Koehler, "Proton beam irradiation of uveal melanomas. Results of 5 1/2-year study," Arch. Ophthalmol. **100**, 928–934 (1982).
[7]E. S. Gragoudas, A. M. Lane, J. Munzenrider, K. M. Egan, and W. Li, "Long-term risk of local failure after proton therapy for choroidal/ciliary body melanoma," Trans. Am. Ophthalmol. Soc. **100**, 43–48 (discussion 48–49) (2002).
[8]J. L. Hungerford, A. J. Foss, I. Whelahan, R. D. Errington, A. Kacperek, and J. Kongerud, "Side effects of photon and proton radiotherapy for ocular melanoma," Front. Radiat. Ther. Oncol. **30**, 287–293 (1997).
[9]M. W. Wilson and J. L. Hungerford, "Comparison of episcleral plaque and proton beam radiation therapy for the treatment of choroidal melanoma," Ophthalmology **106**, 1579–1587 (1999).
[10]D. H. Char, S. M. Kroll, and J. Castro, "Ten-year follow-up of helium ion therapy for uveal melanoma," Am. J. Ophthalmol. **125**, 81–89 (1998).
[11]C. M. Schirmer, M. Chan, J. Mignano, J. Duker, C. S. Melhus, L. B. Williams, J. K. Wu, and K. C. Yao, "Dose de-escalation with gamma knife radiosurgery in the treatment of choroidal melanoma," Int. J. Radiat. Oncol., Biol., Phys. **75**, 170–176 (2009).
[12]P. T. Finger, K. J. Chin, G. P. Yu, and N. S. Patel, "Risk factors for cataract after palladium-103 ophthalmic plaque radiation therapy," Int. J. Radiat. Oncol., Biol., Phys. **80**, 800–806 (2010).
[13]P. T. Finger, "Tumour location affects the incidence of cataract and retinopathy after ophthalmic plaque radiation therapy," Br. J. Ophthalmol. **84**, 1068–1070 (2000).
[14]P. Finger and A. Murphree, "Ophthalmic brachytherapy: Treatment of choroidal melanoma and retinoblastoma," in *Vitreoretinal Surgical Techniques*, edited by G. Peyman, S. Meffert, M. Conway, and F. Chou (Martin Dunitz, London, 2001), pp. 403–418.
[15]Collaborative Ocular Melanoma Study Group, "Design and methods of a clinical trial for a rare condition: The Collaborative Ocular Melanoma Study: COMS Report No. 3," Control Clin. Trials **14**, 362–391 (1993).
[16]B. S. Hawkins, "The Collaborative Ocular Melanoma Study (COMS) randomized trial of pre-enucleation radiation of large choroidal melanoma: IV. Ten-year mortality findings and prognostic factors: COMS Report No. 24," Am. J. Ophthalmol. **138**, 936–951 (2004).
[17]J. Earle, R. W. Kline, and D. M. Robertson, "Selection of iodine 125 for the Collaborative Ocular Melanoma Study," Arch. Ophthalmol. **105**, 763–764 (1987).
[18]S. Packer, S. Stoller, M. L. Lesser, F. S. Mandel, and P. T. Finger, "Long-term results of iodine 125 irradiation of uveal melanoma," Ophthalmology **99**, 767–773 (discussion 774) (1992).
[19]Collaborative Ocular Melanoma Study Group, "The COMS randomized trial of iodine 125 brachytherapy for choroidal melanoma: V. Twelve-year mortality rates and prognostic factors: COMS Report No. 28," Arch. Ophthalmol. **124**, 1684–1693 (2006).
[20]R. W. Kline and J. Earle, "Implications of TG-43 for dose prescription and calculation for I-125 eye plaques," Med. Phys. **23**, 1054 (1996).
[21]W. Hanson, "Implementation of the new I-125 standard and TG-43 recommendations in a cooperative clinical trial," Med. Phys. **23**, 1054 (1996).
[22]S. K. Ray, R. Bhatnagar, W. F. Hartsell, and G. R. Desai, "Review of eye plaque dosimetry based on AAPM Task Group 43 recommendations. American Association of Physicists in Medicine," Int. J. Radiat. Oncol., Biol., Phys. **41**, 701–706 (1998).
[23]R. Nath, L. L. Anderson, G. Luxton, K. A. Weaver, J. F. Williamson, and A. S. Meigooni, "Dosimetry of interstitial brachytherapy sources: Recommendations of the AAPM Radiation Therapy Committee Task Group No. 43. American Association of Physicists in Medicine," Med. Phys. **22**, 209–234 (1995) [see comment: erratum appears in Med. Phys. **23**(9), 1579 (1996)].
[24]Collaborative Ocular Melanoma Study Group, "Radiation therapy," in *COMS Manual of Procedures PB95-179693*, edited by N. T. I. Service (National Technical Information Service, Springfield, VA, 1995), Chap. 12.
[25]R. W. Kline and P. D. Yeakel, "Ocular melanoma, I-125 plaques," Med. Phys. **14**, 475 (1987).

[26]S. T. Chiu-Tsao, L. L. Anderson, K. O'Brien, L. Stabile, and J. C. Liu, "Dosimetry for ^{125}I seed (model 6711) in eye plaques," Med. Phys. **20**, 383–389 (1993).
[27]M. J. Rivard, B. M. Coursey, L. A. DeWerd, W. F. Hanson, M. S. Huq, G. S. Ibbott, M. G. Mitch, R. Nath, and J. F. Williamson, "Update of AAPM Task Group No. 43 Report: A revised AAPM protocol for brachytherapy dose calculations," Med. Phys. **31**, 633–674 (2004) [see comment: erratum appears in Med. Phys. **31**(12), 3532–3533 (2004)].
[28]J. F. Williamson, B. M. Coursey, L. A. DeWerd, W. F. Hanson, R. Nath, and G. Ibbott, "Guidance to users of Nycomed Amersham and North American Scientific, Inc., I-125 interstitial sources. Dosimetry and calibration changes: Recommendations of the American Association of Physicists in Medicine Radiation Therapy Committee Ad Hoc Subcommittee on low-energy seed dosimetry," Med. Phys. **26**, 570–573 (1999).
[29]S. M. Seltzer, P. J. Lamperti, R. Loevinger, C. G. Soares, and J. T. Weaver, "New NIST air-kerma strength standards for I-125 and Pd-103 brachytherapy seeds," Med. Phys. **25**, A170 (1998).
[30]M. J. Rivard, W. M. Butler, L. A. DeWerd, M. S. Huq, G. S. Ibbott, A. S. Meigooni, C. S. Melhus, M. G. Mitch, R. Nath, and J. F. Williamson, "Supplement to the 2004 update of the AAPM Task Group No. 43 Report," Med. Phys. **34**, 2187–2205 (2007).
[31]R. E. Taylor and D. W. Rogers, "An EGSnrc Monte Carlo-calculated database of TG-43 parameters," Med. Phys. **35**, 4228–4241 (2008).
[32]J. Dolan, Z. Lia, and J. F. Williamson, "Monte Carlo and experimental dosimetry of an ^{125}I brachytherapy seed," Med. Phys. **33**, 4675–4684 (2006).
[33]J. I. Monroe and J. F. Williamson, "Monte Carlo-aided dosimetry of the theragenics TheraSeed model 200 103Pd interstitial brachytherapy seed," Med. Phys. **29**, 609–621 (2002).
[34]M. J. Rivard, "Monte Carlo radiation dose simulations and dosimetric comparison of the model 6711 and 9011 ^{125}I brachytherapy sources," Med. Phys. **36**, 486–491 (2009).
[35]R. E. Taylor and D. W. Rogers, "More accurate fitting of ^{125}I and ^{103}Pd radial dose functions," Med. Phys. **35**, 4242–4250 (2008).
[36]J. F. Williamson, W. Butler, L. A. Dewerd, M. S. Huq, G. S. Ibbott, M. G. Mitch, R. Nath, M. J. Rivard, D. Todor, "Recommendations of the American Association of Physicists in Medicine regarding the impact of implementing the 2004 Task Group 43 report on dose specification for ^{103}Pd and ^{125}I interstitial brachytherapy," Med. Phys. **32**, 1424–1439 (2005).
[37]J. F. Williamson, B. M. Coursey, L. A. DeWerd, W. F. Hanson, R. Nath, M. J. Rivard, and G. Ibbott, "Recommendations of the American Association of Physicists in Medicine on ^{103}Pd interstitial source calibration and dosimetry: Implications for dose specification and prescription," Med. Phys. **27**, 634–642 (2000).
[38]S. Nag, J. M. Quivey, J. D. Earle, D. Followill, J. Fontanesi, and P. T. Finger, "The American Brachytherapy Society recommendations for brachytherapy of uveal melanomas," Int. J. Radiat. Oncol., Biol., Phys. **56**, 544–555 (2003).
[39]M. Rotman, S. Packer, J. L. Bosworth, and S. T. Chiu-Tsao, "^{125}I ophthalmic applicators in the treatment of choroidal melanoma," Int. J. Radiat. Oncol., Biol., Phys. **10**(2), 107–108 (1984).
[40]C. Karolis, R. B. Frost, and F. A. Billson, "A thin I-125 seed eye plaque to treat intraocular tumors using an acrylic insert to precisely position the sources," Int. J. Radiat. Oncol., Biol., Phys. **18**, 1209–1213 (1990).
[41]J. C. Hill, R. Sealy, D. Shackleton, C. Stannard, J. Korrubel, E. Hering, and C. Loxton, "Improved iodine-125 plaque design in the treatment of choroidal malignant melanoma," Br. J. Ophthalmol. **76**, 91–94 (1992).
[42]R. Sealy, P. L. le Roux, F. Rapley, E. Hering, D. Shackleton, and D. Sevel, "The treatment of ophthalmic tumours with low-energy sources," Br. J. Radiol. **49**, 551–554 (1976).
[43]M. A. Astrahan, G. Luxton, Q. Pu, and Z. Petrovich, "Conformal episcleral plaque therapy," Int. J. Radiat. Oncol., Biol., Phys. **39**, 505–519 (1997).
[44]W. G. Cross, J. Hokkanen, H. Jarvinen, F. Mourtada, P. Sipila, C. G. Soares, and S. Vynckier, "Calculation of beta-ray dose distributions from ophthalmic applicators and comparison with measurements in a model eye," Med. Phys. **28**, 1385–1396 (2001).
[45]C. G. Soares, S. Vynckier, H. Jarvinen, W. G. Cross, P. Sipila, D. Fluhs, B. Schaeken, F. A. Mourtada, G. A. Bass, and T. T. Williams, "Dosimetry of beta-ray ophthalmic applicators: Comparison of different measurement methods," Med. Phys. **28**, 1373–1384 (2001).
[46]S. Nag, D. Wang, H. Wu, C. J. Bauer, R. B. Chambers, and F. H. Davidorf, "Custom-made "Nag" eye plaques for ^{125}I brachytherapy," Int. J. Radiat. Oncol., Biol., Phys. **56**, 1373–1380 (2003).
[47]C. L. Shields, M. Naseripour, J. Cater, J. A. Shields, H. Demirci, A. Youseff, and J. Freire, "Plaque radiotherapy for large posterior uveal melanomas (> or = 8-mm thick) in 354 consecutive patients," Ophthalmology **109**, 1838–1849 (2002).
[48]I. Puusaari, J. Heikkonen, and T. Kivela, "Effect of radiation dose on ocular complications after iodine brachytherapy for large uveal melanoma: Empirical data and simulation of collimating plaques," Invest. Ophthalmol. Visual Sci. **45**, 3425–3434 (2004).
[49]D. Granero, J. Perez-Calatayud, F. Ballester, E. Casal, and J. M. de Frutos, "Dosimetric study of the 15 mm ROPES eye plaque," Med. Phys. **31**, 3330–3336 (2004).
[50]M. A. Astrahan, A. Szechter, and P. T. Finger, "Design and dosimetric considerations of a modified COMS plaque: The reusable "seed-guide" insert," Med. Phys. **32**, 2706–2716 (2005).
[51]P. T. Finger, "Finger's "slotted" eye plaque for radiation therapy: Treatment of juxtapapillary and circumpapillary intraocular tumours," Br. J. Ophthalmol. **91**, 891–894 (2007).
[52]G. Luxton, M. A. Astrahan, P. E. Liggett, D. L. Neblett, D. M. Cohen, and Z. Petrovich, "Dosimetric calculations and measurements of gold plaque ophthalmic irradiators using iridium-192 and iodine-125 seeds," Int. J. Radiat. Oncol., Biol., Phys. **15**, 167–176 (1988).
[53]R. M. Thomson, K. M. Furutani, J. S. Pulido, S. L. Stafford, and D. W. O. Rogers, "Modified COMS plaques for ^{125}I and ^{103}Pd iris melanoma brachytherapy," Int. J. Radiat. Oncol., Biol., Phys. **78**, 1261–1269 (2010).
[54]S. Packer and M. Rotman, "Radiotherapy of choroidal melanoma with iodine-125," Ophthalmology **87**, 582–590 (1980).
[55]M. C. Schell, K. A. Weaver, T. L. Phillips, D. H. Char, J. M. Quivey, C. Barnett, and C. C. Ling, "Design of iodine-125 eye plaques for radiation therapy," Endocurie Hypertherm Oncol. **5**, 83–90 (1989).
[56]A. K. Vine, R. K. Randall, K. TenHaken, R. F. Diaz, B. B. Maxson, and A. S. Lichter, "A new inexpensive customized plaque for choroidal melanoma iodine-125 plaque therapy," Ophthalmology **96**, 543–546 (1989).
[57]P. T. Finger, K. J. Chin, and L. B. Tena, "A five-year study of slotted plaque radiation therapy for choroidal melanoma: Near, touching or surrounding the optic nerve," Ophthalmology **119**, 415–422 (2012).
[58]http://www.aapm.org/pubs/reports/RPT_129.pdf.
[59]R. M. Thomson, R. E. Taylor, and D. W. O. Rogers, "Monte Carlo dosimetry for ^{125}I and ^{103}Pd eye plaque brachytherapy," Med. Phys. **35**, 5530–5543 (2008).
[60]A. Wu and F. Krasin, "Film dosimetry analyses on the effect of gold shielding for iodine-125 eye plaque therapy for choroidal melanoma," Med. Phys. **17**, 843–846 (1990).
[61]R. W. Kline, "Notes regarding seed coordinates for COMS eye plaques," 2011, see http://rpc.mdanderson.org/rpc/credentialing/Notes - COMS Eye Plaques 2002.doc.
[62]A. de la Zerda, S. T. Chiu-Tsao, J. Lin, L. L. Boulay, I. Kanna, J. H. Kim, and H. S. Tsao, "^{125}I eye plaque dose distribution including penumbra characteristics," Med. Phys. **23**, 407–418 (1996).
[63]K. A. Weaver, "The dosimetry of 125I seed eye plaques," Med. Phys. **13**, 78–83 (1986).
[64]A. N. Harnett and E. S. Thomson, "An iodine-125 plaque for radiotherapy of the eye: Manufacture and dosimetric considerations," Br. J. Radiol. **61**, 835–838 (1988).
[65]W. Alberti, B. Pothmann, P. Tabor, K. Muskalla, K. P. Hermann, and D. Harder, "Dosimetry and physical treatment planning for iodine eye plaque therapy," Int. J. Radiat. Oncol., Biol., Phys. **20**, 1087–1092 (1991).
[66]A. Wu, E. S. Sternick, and D. J. Muise, "Effect of gold shielding on the dosimetry of an ^{125}I seed at close range," Med. Phys. **15**, 627–628 (1988).
[67]S. T. Chiu-Tsao, L. Bouley, I. Kanna, A. Zerda, and J. H. Kim, "Dose distribution in the eye for ^{103}Pd COMS eye plaque," Med. Phys. **22**, 923 (1995).
[68]J. Cygler, J. Szanto, M. Soubra, and D. W. Rogers, "Effects of gold and silver backings on the dose rate around an ^{125}I seed," Med. Phys. **17**, 172–178 (1990).
[69]J. A. Meli and K. A. Motakabbir, "The effect of lead, gold, and silver backings on dose near ^{125}I seeds," Med. Phys. **20**, 1251–1256 (1993).

[70]S. Knutsen, R. Hafslund, O. R. Monge, H. Valen, L. P. Muren, B. L. Rekstad, J. Krohn, and O. Dahl, "Dosimetric verification of a dedicated 3D treatment planning system for episcleral plaque therapy," Int. J. Radiat. Oncol., Biol., Phys. **51**, 1159–1166 (2001).
[71]M. P. Casebow, "The calculation and measurement of exposure distributions from 60 Co ophthalmic applicators," Br. J. Radiol. **44**, 618–624 (1971).
[72]G. Taccini, F. Cavagnetto, G. Coscia, S. Garelli, and A. Pilot, "The determination of dose characteristics of ruthenium ophthalmic applicators using radiochromic film," Med. Phys. **24**, 2034–2037 (1997).
[73]A. Krintz, W. F. Hanson, G. S. Ibbott, and D. S. Followill, "Verification of plaque simulator dose distributions using radiochromic film," Med. Phys. **29**, 1220–1221 (2002, abstract).
[74]A. L. Krintz, W. F. Hanson, G. S. Ibbott, and D. S. Followill, "A reanalysis of the Collaborative Ocular Melanoma Study Medium Tumor Trial eye plaque dosimetry," Int. J. Radiat. Oncol., Biol., Phys. **56**, 889–898 (2003).
[75]H. Acar, "Verification of Plaque Simulator dose distributions using GAFCHROMIC® EBT film," Türk Onkoloji Dergisi **25**, 150–156 (2010).
[76]D. Fluhs, M. Heintz, F. Indenkampen, and C. Wieczorek, "Direct reading measurement of absorbed dose with plastic scintillators: The general concept and applications to ophthalmic plaque dosimetry," Med. Phys. **23**, 427–304 (1996).
[77]A. S. Kirov, J. Z. Piao, N. K. Mathur, T. R. Miller, S. Devic, S. Trichter, M. Zaider, C. G. Soares, and T. LoSasso, "The three-dimensional scintillation dosimetry method: Test for a ^{106}Ru eye plaque applicator," Phys. Med. Biol. **50**, 3063–3081 (2005).
[78]M. F. Chan, A. Y. Fung, Y. C. Hu, C. S. Chui, H. Amols, M. Zaider, and D. Abramson, "The measurement of three dimensional dose distribution of a ruthenium-106 ophthalmological applicator using magnetic resonance imaging of BANG polymer gels," J. Appl. Clin. Med. Phys. **2**, 85–89 (2001).
[79]M. A. Astrahan, "Improved treatment planning for COMS eye plaques," Int. J. Radiat. Oncol., Biol., Phys. **61**, 1227–1242 (2005).
[80]J. Hokkanen, J. Heikkonen, and P. Holmberg, "Theoretical calculations of dose distributions for beta-ray eye applicators," Med. Phys. **24**, 211–213 (1997).
[81]B. Chan, M. Rotman, and G. J. Randall, "Computerized dosimetry of ^{60}Co ophthalmic applicators," Radiology **103**, 705–707 (1972).
[82]C. S. Melhus and M. J. Rivard, "COMS eye plaque brachytherapy dosimetry simulations for ^{103}Pd, ^{125}I, and ^{131}Cs," Med. Phys. **35**, 3364–3371 (2008).
[83]R. M. Thomson and D. W. O. Rogers, "Monte Carlo dosimetry for ^{125}I and ^{103}Pd eye plaque brachytherapy with various seed models," Med. Phys. **37**, 368–376 (2010).
[84]S. T. Chiu-Tsao, K. O'Brien, R. Sanna, H. S. Tsao, C. Vialotti, Y. S. Chang, M. Rotman, and S. Packer, "Monte Carlo dosimetry for ^{125}I and ^{60}Co in eye plaque therapy," Med. Phys. **13**, 678–682 (1986).
[85]F. Mourtada, N. Koch, and W. Newhauser, "^{106}Ru/^{106}Rh plaque and proton radiotherapy for ocular melanoma: A comparative dosimetric study," Radiat. Prot. Dosimetry **116**, 454–460 (2005).
[86]H. Zhang, D. Martin, S. T. Chiu-Tsao, A. Meigooni, and B. R. Thomadsen, "A comprehensive dosimetric comparison between ^{131}Cs and ^{125}I brachytherapy sources for COMS eye plaque implant," Brachytherapy **9**, 362–372 (2010).
[87]K. Gifford, S. Kirsner, J. Horton, T. Wareing, and F. Mourtada, "Calculation of the dose distribution around a commercially available ^{125}I brachytherapy source via a multi-group discrete ordinates," Med. Phys. **34**, 2550 (2007).
[88]J. Bristol, "Comparison of eye plaque dosimetry using deterministic and Monte Carlo methods," M.S. thesis, Oregon State University, 2010.
[89]M. J. Rivard, C. S. Melhus, S. Sioshansi, and J. Morr, "The impact of prescription depth, dose rate, plaque size, and source loading on the central axis using ^{103}Pd, ^{125}I, and ^{131}Cs," Brachytherapy **7**, 327–335 (2008).
[90]M. J. Rivard, S.-T. Chiu-Tsao, P. T. Finger, A. S. Meigooni, C. S. Melhus, F. Mourtada, M. E. Napolitano, D. W. O. Rogers, R. M. Thomson, and R. Nath, "Comparison of dose calculation methods for brachytherapy of intraocular tumors," Med. Phys. **38**, 306–316 (2011).
[91]G. Luxton, M. A. Astrahan, and Z. Petrovich, "Backscatter measurements from a single seed of ^{125}I for opthalmic plaque dosimetry," Med. Phys. **15**, 397–400 (1988).
[92]M. J. Rivard, C. S. Melhus, D. Granero, J. Perez-Calatayud, and F. Ballester, "An approach to using conventional brachytherapy software for clinical treatment planning of complex, Monte Carlo-based brachytherapy dose distributions," Med. Phys. **36**, 1968–1975 (2009).
[93]M. J. Rivard, L. Beaulieu, and F. Mourtada, "Enhancements to commissioning techniques and quality assurance of brachytherapy treatment planning systems that use model-based dose calculation algorithms," Med. Phys. **37**, 2645–2658 (2010).
[94]A. Carlsson Tedgren and A. Ahnesjo, "Optimization of the computational efficiency of a 3D, collapsed cone dose calculation algorithm for brachytherapy," Med. Phys. **35**, 1611–1618 (2008).
[95]A. K. Tedgren and A. Ahnesjo, "Accounting for high Z shields in brachytherapy using collapsed cone superposition for scatter dose calculation," Med. Phys. **30**, 2206–2217 (2003).
[96]B. R. Thomadsen, J. F. Williamson, M. J. Rivard, and A. S. Meigooni, "Anniversary paper: Past and current issues, and trends in brachytherapy physics," Med. Phys. **35**, 4708–4723 (2008).
[97]M. J. Rivard, J. L. Venselaar, and L. Beaulieu, "The evolution of brachytherapy treatment planning," Med. Phys. **36**, 2136–2153 (2009).
[98]M. J. Rivard, W. M. Butler, P. M. Devlin, J. K. Hayes, Jr., R. A. Hearn, E. P. Lief, A. S. Meigooni, G. S. Merrick, and J. F. Williamson, "American Brachytherapy Society recommends no change for prostate permanent implant dose prescriptions using iodine-125 or palladium-103," Brachytherapy **6**, 34–37 (2007).
[99]http://rpc.mdanderson.org/RPC/BrachySeeds/Source_Registry.htm.
[100]http://www.estro.org/estroactivities/Pages/GEC-BRACHYTHERAPYCOMMITTEEACTIVITY.aspx.
[101]http://www.physics.carleton.ca/clrp/seed_database.
[102]M. D. Evans, M. A. Astrahan, and R. Bate, "Tumor localization using fundus view photography for episcleral plaque therapy," Med. Phys. **20**, 769–775 (1993).
[103]A. G. Kepka, P. M. Johnson, and R. W. Kline, "The generalized geometry of eye plaque therapy," Med. Phys. **15**, 375–379 (1988).
[104]M. A. Astrahan, G. Luxton, G. Jozsef, T. D. Kampp, P. E. Liggett, M. D. Sapozink, and Z. Petrovich, "An interactive treatment planning system for ophthalmic plaque radiotherapy," Int. J. Radiat. Oncol., Biol., Phys. **18**, 679–687 (1990).
[105]S. Chiu-Tsao, "Episcleral eye plaques for treatment of intraocular malignancies," in *Brachytherapy Physics*, edited by B. Thomadsen, M. Rivard, and W. Butler (Medical Physics Publishing, Madison, WI, 2005), pp. 673–705.
[106]Collaborative Ocular Melanoma Study Group, "Echography (ultrasound) procedures for the Collaborative Ocular Melanoma Study Report No. 12," J. Ophthalmic Nurs. Technol. **18**, 219–232 (1999).
[107]J. M. Romero, P. T. Finger, R. B. Rosen, and R. Iezzi, "Three-dimensional ultrasound for the measurement of choroidal melanomas," Arch. Ophthalmol. **119**, 1275–1282 (2001).
[108]P. Schueller, A. Dogan, J. E. Panke, O. Micke, and N. Willich, "Does the imaging method have an influence on the measured tumor height in ruthenium plaque therapy of uveal melanoma?" Strahlenther. Onkol. **181**, 320–325 (2005).
[109]P. V. Houdek, J. G. Schwade, A. J. Medina, C. A. Poole, K. R. Olsen, D. H. Nicholson, S. Byrne, R. Quencer, R. S. Hinks, and V. Pisciotta, "MR technique for localization and verification procedures in episcleral brachytherapy," Int. J. Radiat. Oncol., Biol., Phys. **17**, 1111–1114 (1989).
[110]Collaborative Ocular Melanoma Study Group, "Examination procedures," in *COMS manual of Procedures PB95-179693*, edited by N. T. I. Service (National Technical Information Service, Springfield, VA, 1995), Chap. 9.
[111]T. A. Rice, "personal communication" (1987).
[112]R. W. Kline, "personal communication" (1987).
[113]R. W. Kline, 2011, see http://rpc.mdanderson.org/rpc/credentialing/Coordinate Localization.doc.
[114]M. M. Goodsitt, P. L. Carson, S. Witt, D. L. Hykes, and J. M. Kofler, Jr., "Real-time B-mode ultrasound quality control test procedures: Report of AAPM Ultrasound Task Group No. 1," Med. Phys. **25**, 1385–1406 (1998).
[115]W. M. Butler, W. S. Bice, Jr., L. A. DeWerd, J. M. Hevezi, M. S. Huq, G. S. Ibbott, J. R. Palta, M. J. Rivard, J. P. Seuntjens, and B. R. Thomadsen, "Third-party brachytherapy source calibrations and physicist responsibilities: Report of the AAPM Low Energy Brachytherapy Source Calibration Working Group," Med. Phys. **35**, 3860–3865 (2008).

[116]J. F. Williamson, B. M. Coursey, L. A. DeWerd, W. F. Hanson, R. Nath, M. J. Rivard, and G. Ibbott, "On the use of apparent activity (Aapp) for treatment planning of 125I and 103Pd interstitial brachytherapy sources: Recommendations of the American Association of Physicists in Medicine radiation therapy committee subcommittee on low-energy brachytherapy source dosimetry," Med. Phys. **26**, 2529–2530 (1999).
[117]G. J. Kutcher *et al.*, "Comprehensive QA for radiation oncology: Report of AAPM Radiation Therapy Committee Task Group 40," Med. Phys. **21**, 581–618 (1994).
[118]B. Fraass, K. Doppke, M. Hunt, G. Kutcher, G. Starkschall, R. Stern, and J. Van Dyke, "American Association of Physicists in Medicine Radiation Therapy Committee Task Group 53: Quality assurance for clinical radiotherapy treatment planning," Med. Phys. **25**, 1773–1829 (1998).
[119]A. Beiki-Ardakani, J. Jezioranski, D. A. Jaffray, and I. Young, "Improving quality assurance for assembled COMS eye plaques using a pinhole gamma camera," Med. Phys. **35**, 4318–4323 (2008).
[120]A. Almony, S. Breit, H. Zhao, J. Garcia-Ramirez, D. B. Mansur, and J. W. Harbour, "Tilting of radioactive plaques after initial accurate placement for treatment of uveal melanoma," Arch. Ophthalmol. **126**, 65–70 (2008).
[121]J. W. Harbour, T. G. Murray, S. F. Byrne, J. R. Hughes, E. K. Gendron, F. J. Ehlies, and A. M. Markoe, "Intraoperative echographic localization of iodine 125 episcleral radioactive plaques for posterior uveal melanoma," Retina **16**, 129–134 (1996).
[122]P. T. Finger, J. M. Romero, R. B. Rosen, R. Iezzi, R. Emery, and A. Berson, "Three-dimensional ultrasonography of choroidal melanoma: Localization of radioactive eye plaques," Arch. Ophthalmol. **116**, 305–312 (1998).
[123]NRC Regulatory Guide NUREG-1556, "Consolidated guidance about materials licenses: Program-specific guidance about medical licenses," Vol. 9, Rev. 2, 2008, see http://www.nrc.gov/reading-rm/doc-collections/nuregs/staff/sr1556/v9/r2/.
[124]T. W. Kaulich and M. Bamberg, "Radiation protection of persons living close to patients with radioactive implants" Strahlenther. Onkol. **186**, 107–112 (2010).
[125]P. T. Finger, K. J. Chin, and G. Duvall, "Palladium-103 ophthalmic plaque radiation therapy for choroidal melanoma: 400 treated patients," Ophthalmology **116**, 790–796 (2009).
[126]A. Aizman, P. T. Finger, U. Shabto, A. Szechter, and A. Berson, "Palladium 103 (103Pd) plaque radiation therapy for circumscribed choroidal hemangioma with retinal detachment," Arch. Ophthalmol. **122**, 1652–1656 (2004).
[127]P. A. Saconn, C. J. Gee, C. M. Greven, T. P. McCoy, K. E. Ekstrand, and K. M. Greven, "Alternative dose for choroidal melanoma treated with an iodine-125 radioactive plaque: A single-institution retrospective study," Int. J. Radiat. Oncol., Biol., Phys. **78**, 844–848 (2009).
[128]S. Edge, D. Byrd, C. Compton, A. Fritz, F. Greene, and A. Trotti, "Malignant melanoma of the uvea," in *Ophthalmic Sites: Part X, The AJCC Cancer Staging Manual* (Springer, New York, 2009), pp. 547–559.
[129]N. L. Gagne, K. L. Leonard, K. E. Huber, J. E. Mignano, J. S. Duker, N. V. Laver, and M. J. Rivard, "BEDVH - A method for evaluating biologically effective dose volume histograms: Application to eye plaque brachytherapy implants," Med. Phys. **39**, 976–983 (2012).
[130]N. L. Gagne, K. L. Leonard, and M. J. Rivard, "Radiobiology for eye plaque brachytherapy and evaluation of implant duration and radionuclide choice using an objective function," Med. Phys. **39**, 3332–3342 (2012).
[131]U. Schneider, F. Gelisken, W. Inhoffen, and I. Kreissig, "Indocyanine green videoangiography of malignant melanomas of the choroid using the scanning laser ophthalmoscope," Ger. J. Ophthalmol. **5**, 6–11 (1996).
[132]T. H. Pettit, A. Barton, R. Y. Foos, and R. E. Christensen, "Fluorescein angiography of choroidal melanomas," Arch. Ophthalmol. **83**, 27–38 (1970).
[133]H. Newman, K. J. Chin, and P. T. Finger, "Subfoveal choroidal melanoma: Pretreatment characteristics and response to plaque radiation therapy," Arch. Ophthalmol. **129**, 892–898 (2010).
[134]P. T. Finger, K. J. Chin, and G. P. Yu, "Risk factors for radiation maculopathy after ophthalmic plaque radiation for choroidal melanoma," Am. J. Ophthalmol. **149**, 608–615 (2010).
[135]H. Newman, P. T. Finger, K. J. Chin, and A. C. Pavlick, "Systemic bevacizumab (Avastin) for exudative retinal detachment secondary to choroidal melanoma," Eur. J. Ophthalmol. **21**(6), 796–801 (2011).
[136]P. T. Finger and M. Kurli, "Laser photocoagulation for radiation retinopathy after ophthalmic plaque radiation therapy," Br. J. Ophthalmol. **89**(6), 730–738 (2005).
[137]P. T. Finger, "Anti-VEGF bevacizumab (Avastin) for radiation optic neuropathy," Am. J. Ophthalmol. **143**, 335–338 (2007).
[138]P. T. Finger, "Radiation retinopathy is treatable with anti-vascular endothelial growth factor bevacizumab (Avastin)," Int. J. Radiat. Oncol., Biol., Phys. **70**, 974–977 (2008).
[139]P. T. Finger and K. J. Chin, "Intravitreous ranibizumab (lucentis) for radiation maculopathy," Arch. Ophthalmol. **128**, 249–252 (2010).
[140]P. T. Finger and K. Chin, "Anti-vascular endothelial growth factor bevacizumab (avastin) for radiation retinopathy," Arch. Ophthalmol. **125**(6), 751–756 (2007).
[141]P. T. Finger and K. J. Chin, "Antivascular endothelial growth factor bevacizumab for radiation optic neuropathy: Secondary to plaque radiotherapy," Int. J. Radiat. Oncol., Biol., Phys. **82**, 789–798 (2012).
[142]P. K. Lommatzsch and R. Lommatzsch, "Treatment of juxtapapillary melanomas," Br. J. Ophthalmol. **75**, 715–717 (1991).
[143]P. K. Lommatzsch, C. Werschnik, and E. Schuster, "Long-term follow-up of Ru-106/Rh-106 brachytherapy for posterior uveal melanoma," Graefe's Arch. Clin. Exp. Ophthalmol. **238**, 129–137 (2000).
[144]J. Fontanesi, D. Meyer, S. Xu, and D. Tai, "Treatment of choroidal melanoma with I-125 plaque," Int. J. Radiat. Oncol., Biol., Phys. **26**, 619–623 (1993).
[145]P. T. Finger, D. Lu, A. Buffa, D. S. DeBlasio, and J. L. Bosworth, "Palladium-103 versus iodine-125 for ophthalmic plaque radiotherapy," Int. J. Radiat. Oncol., Biol., Phys. **27**, 849–854 (1993).
[146]P. T. Finger, D. M. Moshfeghi, and T. K. Ho, "Palladium 103 ophthalmic plaque radiotherapy," Arch. Ophthalmol. **109**, 1610–1613 (1991).
[147]S. Packer, M. Rotman, R. G. Fairchild, D. M. Albert, H. L. Atkins, and B. Chan, "Irradiation of choroidal melanoma with iodine 125 ophthalmic plaque," Arch. Ophthalmol. **98**, 1453–1457 (1980).
[148]D. M. Robertson, K. S. Fountain, J. A. Anderson, and G. W. Posthumus, "Radioactive iodine-125 as a therapeutic radiation source for management of intraocular tumors," Trans. Am. Ophthalmol. Soc. **79**, 294–306 (1981).
[149]B. R. Garretson, D. M. Robertson, and J. D. Earle, "Choroidal melanoma treatment with iodine 125 brachytherapy," Arch. Ophthalmol. **105**, 1394–1397 (1987).
[150]H. C. Boldt, B. M. Melia, J. C. Liu, and S. M. Reynolds, "I-125 brachytherapy for choroidal melanoma photographic and angiographic abnormalities: The Collaborative Ocular Melanoma Study: COMS Report No. 30," Ophthalmology **116**, 106–115 (2009).
[151]M. Melia, C. S. Moy, S. M. Reynolds, J. A. Hayman, T. G. Murray, K. R. Hovland, J. D. Earle, N. Kurinij, L. M. Dong, P. H. Miskala, C. Fountain, D. Cella, and C. M. Mangione, "Quality of life after iodine 125 brachytherapy vs enucleation for choroidal melanoma: 5-year results from the Collaborative Ocular Melanoma Study: COMS QOLS Report No. 3," Arch. Ophthalmol. **124**, 226–238 (2006).
[152]L. Bergman, B. Nilsson, G. Lundell, M. Lundell, and S. Seregard, "Ruthenium brachytherapy for uveal melanoma, 1979–2003: Survival and functional outcomes in the Swedish population," Ophthalmology **112**, 834–840 (2005).
[153]B. Damato, I. Patel, I. R. Campbell, H. M. Mayles, and R. D. Errington, "Local tumor control after ^{106}Ru brachytherapy of choroidal melanoma," Int. J. Radiat. Oncol., Biol., Phys. **63**, 385–391 (2005).
[154]B. Damato, I. Patel, I. R. Campbell, H. M. Mayles, and R. D. Errington, "Visual acuity after Ruthenium(106) brachytherapy of choroidal melanomas," Int. J. Radiat. Oncol., Biol., Phys. **63**, 392–400 (2005).
[155]B. F. Fernandes, H. Krema, E. Fulda, C. J. Pavlin, D. G. Payne, H. D. McGowan, and E. R. Simpson, "Management of iris melanomas with 125Iodine plaque radiotherapy," Am. J. Ophthalmol. **149**, 70–76 (2010).
[156]R. Potter, K. Janssen, F. J. Prott, J. Widder, U. Haverkamp, H. Busse, and R. P. Muller, "Ruthenium-106 eye plaque brachytherapy in the conservative treatment of uveal melanoma: Evaluation of 175 patients treated with 150 Gy from 1981–1989," Front. Radiat. Ther. Oncol. **30**, 143–149 (1997).
[157]S. Seregard, "Long-term survival after ruthenium plaque radiotherapy for uveal melanoma: A meta-analysis of studies including 1066 patients," Acta Ophthalmol. Scand. **77**, 414–417 (1999).
[158]P. Isager, N. Ehlers, S. F. Urbak, and J. Overgaard, "Visual outcome, local tumour control, and eye preservation after ^{106}Ru/Rh brachytherapy for choroidal melanoma," Acta Oncol. **45**, 285–293 (2006).

[159]P. T. Finger, "Plaque radiation therapy for malignant melanoma of the iris and ciliary body," Am. J. Ophthalmol. **132**, 328–335 (2001).
[160]P. T. Finger, S. Reddy, and K. Chin, "High-frequency ultrasound characteristics of 24 iris and iridociliary melanomas: Before and after plaque brachytherapy," Arch. Ophthalmol. **125**, 1051–1058 (2007).
[161]F. A. Marigo, P. T. Finger, S. A. McCormick, R. Iezzi, K. Esaki, H. Ishikawa, J. M. Liebmann, and R. Ritch, "Iris and ciliary body melanomas: Ultrasound biomicroscopy with histopathologic correlation," Arch. Ophthalmol. **118**, 1515–1521 (2000).
[162]F. A. Marigo and P. T. Finger, "Anterior segment tumors: Current concepts and innovations," Surv. Ophthalmol. **48**, 569–593 (2003).
[163]J. P. Garcia, Jr., L. Spielberg, and P. T. Finger, "High-frequency ultrasound measurements of the normal ciliary body and iris," Ophthalmic Surg. Lasers Imaging **42**(4), 321–327 (2011).
[164]C. Shields, M. Naseripour, J. Shields, J. Freir, and J. Cater, "Custom-designed plaque radiotherapy for nonresectable iris melanoma in 38 patients: Tumor control and ocular complications," Am. J. Ophthalmol. **135**, 648–656 (2003).
[165]F. E. Kruse, K. Rohrschneider, and H. E. Volcker, "Transplantation of amniotic membrane for reconstruction of the eye surface," Ophthalmologe **95**, 114–119 (1998).
[166]P. T. Finger, "Finger's amniotic membrane buffer technique: Protecting the cornea during radiation plaque therapy," Arch. Ophthalmol. **126**, 531–534 (2008).
[167]J. P. Garcia, Jr., P. T. Garcia, R. B. Rosen, and P. T. Finger, "A 3-dimensional ultrasound C-scan imaging technique for optic nerve measurements," Ophthalmology **111**, 1238–1243 (2004).
[168]J. W. Harbour, T. A. Meredith, P. A. Thompson, and M. E. Gordon, "Transpupillary thermotherapy versus plaque radiotherapy for suspected choroidal melanomas," Ophthalmology **110**, 2207–2214; discussion 2215 (2003).
[169]N. M. Radcliffe and P. T. Finger, "Eye cancer related glaucoma: Current concepts." Surv. Ophthalmol. **54**(1), 47–73 (2009).
[170]I. Puusaari, J. Heikkonen, and T. Kivela, "Ocular complications after iodine brachytherapy for large uveal melanomas," Ophthalmology **111**, 1768–1777 (2004).
[171]R. M. Conway, A. M. Poothullil, I. K. Daftari, V. Weinberg, J. E. Chung, and J. M. O'Brien, "Estimates of ocular and visual retention following treatment of extra-large uveal melanomas by proton beam radiotherapy," Arch. Ophthalmol. **124**, 838–843 (2006).
[172]J. Sisterson, "Ion beam therapy in 2004," Nucl. Instrum. Methods Phys. Res. B **241**, 713–716 (2005).
[173]A. Courdi, J. P. Caujolle, J. D. Grange, L. Diallo-Rosier, J. Sahel, F. Bacin, C. Zur, P. Gastaud, N. Iborra-Brassart, J. Herault, and P. Chauvel, "Results of proton therapy of uveal melanomas treated in Nice," Int. J. Radiat. Oncol., Biol., Phys. **45**, 5–11 (1999).
[174]E. Egger, L. Zografos, A. Schalenbourg, D. Beati, T. Bohringer, L. Chamot, and G. Goitein, "Eye retention after proton beam radiotherapy for uveal melanoma," Int. J. Radiat. Oncol., Biol., Phys. **55**, 867–880 (2003).
[175]O. Pastyr, G. H. Hartmann, W. Schlegel, S. Schabbert, H. Treuer, W. J. Lorenz, and V. Sturm, "Stereotactically guided convergent beam irradiation with a linear accelerator: Localization-technique," Acta Neurochir. **99**, 61–64 (1989).
[176]K. Muller, P. J. Nowak, C. de Pan, J. P. Marijnissen, D. A. Paridaens, P. Levendag, and G. P. Luyten, "Effectiveness of fractionated stereotactic radiotherapy for uveal melanoma," Int. J. Radiat. Oncol., Biol., Phys. **63**, 116–122 (2005).
[177]K. Dieckmann, J. Bogner, D. Georg, M. Zehetmayer, G. Kren, and R. Potter, "A linac-based stereotactic irradiation technique of uveal melanoma," Radiother. Oncol. **61**, 49–56 (2001).
[178]R. Dunavoelgyi, K. Dieckmann, A. Gleiss, S. Sacu, K. Kircher, M. Georgopoulos, D. Georg, M. Zehetmayer, and R. Poetter, "Local tumor control, visual acuity, and survival after hypofractionated stereotactic photon radiotherapy of choroidal melanoma in 212 patients treated between 1997 and 2007," Int. J. Radiat. Oncol., Biol., Phys. **81**, 199–205 (2011).
[179]P. E. Carvounis and B. Katz, "Gamma knife radiosurgery in neuro-ophthalmology," Curr. Opin. Ophthalmol. **14**, 317–324 (2003).
[180]R. Liscak and V. Vladyka, "Radiosurgery in ocular disorders: Clinical applications," Prog. Neurol. Surg. **20**, 324–339 (2007).
[181]S. Logani, T. K. Helenowski, H. Thakrar, and B. Pothiawala, "Gamma Knife radiosurgery in the treatment of ocular melanoma," Stereotact. Funct. Neurosurg. **61**(Suppl. 1), 38–44 (1993).
[182]G. Marchini *et al.*, "Stereotactic radiosurgery of uveal melanomas: Preliminary results with Gamma Knife treatment," Stereotact. Funct. Neurosurg. **64**(Suppl. 1), 72–79 (1995).
[183]P. Pochop, J. Pilbauer, J. Krepelkova, V. Vladyka, R. Liscak, J. Sach, and G. Simonova, "Two years' experience with treatment of uveal melanoma using the Leksell gamma knife," Cesk. Slov. Oftalmol. **54**, 222–234 (1998).
[184]G. Modorati, E. Miserocchi, L. Galli, P. Picozzi, and P. Rama, "Gamma knife radiosurgery for uveal melanoma: 12 years of experience," Br. J. Ophthalmol. **93**, 40–44 (2009).
[185]S. Trichter, H. Amols, G. N. Cohen, D. Lewis, T. LoSasso, and M. Zaider, "Accurate dosimetry of Ru-106 ophthalmic applicators using GafChromic film in a solid water phantom," Med. Phys. **29**, 1349 (2002).
[186]S. Trichter, M. Zaider, D. Nori, A. Sabbas, F. Kulidzhanov, D. Lewis, and C. Soares, "Clinical dosimetry of 106Ru eye plaques in accordance with the forthcoming ISO beta dosimetry standard using specially designed GAFCHROMIC® Film," Int. J. Radiat. Oncol., Biol., Phys. **69**, S665–S666 (2007).
[187]M. A. Astrahan, "A patch source model for treatment planning of ruthenium ophthalmic applicators," Med. Phys. **30**, 1219–1228 (2003).
[188]ISO 21439, *Clinical Dosimetry-Beta Radiation sources for Brachytherapy* (International Organization for Standardization, 2009).